Alcoholate corrosion of aluminium in ethanol blends

-the effects of water content, surface treatments, temperature, time and pressure

Jenny Linder

Master Thesis in Corrosion Science (KTH Royal Institute of Technology, Div. Surface and Corrosion Science, Stockholm)

Work carried out at Swerea KIMAB, Stockholm

Abstract

As it becomes more important to replace fossil fuels with alternative fuels, biofuels like ethanol are becoming more commercially used. The increased use of ethanol brings good influences such as lower impact on the environment. However, the use of ethanol can also bring negative effects regarding corrosion of metals. In the automotive industry aluminium has been seen affected by a novel very aggressive corrosion phenomenon, alcoholate corrosion. This master thesis investigation has investigated the effect of a few parameters of importance for alcoholate corrosion; water, temperature, time and pressure. The aluminium alloys AA6063 and A380 have been investigated and the capacity of five different surface treatments of AA6063 has been tested to observe if they inhibit the effect of alcoholate corrosion.

Throughout the experiments the water dependence of alcoholate corrosion has showed to be of large importance for the corrosion process. An increase in water content will postpone the start of alcoholate corrosion or prevent corrosion to occur. A correlation between temperature and time has been observed. Higher temperatures results in a shorter time period of exposure before alcoholate corrosion occurs, and vice versa. The effect of different pressures was investigated and showed no effect on alcoholate corrosion when using pressurisation with the inert nitrogen gas.

All surface treatments revealed a capacity to protect the aluminium alloy against alcoholate corrosion to different extent. The electroless nickel plating seemed to prevent alcoholate corrosion while the Keronite coating seemed more sensitive to this form of corrosion.

Summary of content

1 Introduction

1.1 Background

It has become more and more important to use alternative bio-fuels as the fossil fuels are drained, the awareness of lowering the emissions has become more essential and the cost is increasing. Of the biofuels coming out on the market bio-ethanol is an attractive fuel which can be used in the already existing infrastructure. Bio-ethanol blended gasoline of 10% ethanol volume (E10) reduces the cost by approximately 3% and is already in use around the world. E10 is generally seen as the upper bound[1] for what ordinary vehicles can manage before corrosion occur in the engine and fuel systems composed of aluminium. However some reports account for aluminium corroding in E10 and in 2007 Toyota got reports from USA and Thailand of fuel rails corroding.[2-4] Toyotas investigation showed ethanol fuel with low water levels to be the main reason for corrosion to occur, however no underlying mechanisms could be discerned or governing parameters pointed out. Toyota solved the problem by changing the coating on the fuel rails.[3] In Europe, Japan and USA, companies have developed vehicles with engines and fuel systems that can run on fuels with different ethanol volumes up to pure ethanol, E100. These engines and fuel systems are compatible with polymers and stainless steels but presents problems in contact with aluminium. Increasing the ethanol content from E10 to E20 can give even more unpredictable corrosive effects and the issues of corrosion of aluminium need to be addressed.[1]

1.2 Aim

The aim with this master thesis work is to determine how the parameters; water content in ethanol, temperature, time and pressure influence alcoholate corrosion of the aluminium alloy AA6063 in ethanol blended biofuels. Different surface treatments for aluminium alloy AA6063 were also investigated to study their possible inhibiting effect on alcoholate corrosion.

1.3 Theory

1.3.1 Aluminium

Aluminium was discovered in 1809 but it was not until 1827 it was possible to extract sufficient amounts of pure aluminium to distinguish some of its properties. In 1856 the first aluminium plant was established in Paris. The first years the production consisted of around 0.5 tonnes/year and aluminium was more expensive than silver. In the following years the manufacturing process of aluminium has grown and in year 1990, over 19 million tonnes aluminium was produced every year on a world-wide basis.[5]

Pure aluminium can be derived from aluminium oxide which can be found in bauxite. Bauxite is a red soil which mainly consists of aluminium oxide, Al_2O_3, in a mixture of iron oxide, Fe_3O_4, and silica, SiO_2. Aluminium oxide is derived from bauxite but is very stable and hence difficult to reduce to metallic aluminium. Extraction of bauxite to pure aluminium is hence an energy consuming process and aluminium is therefore a relative expensive metal. However with the qualities aluminium possesses, after steel; it gives a high economic value. The numerous advantageous properties of aluminium make it a very attractive material which has led to an increase of the consumption since the 1950´s.

The many advantageous properties of aluminium are for example corrosion resistance, low density, ease to be formed and good thermal conductivity.[5-7] Aluminium and its alloys are therefore used in a wide range of applications. It is consistently used in transport vehicles, such as airplanes, trains and cars[5] and is also used in areas such as household appliances, mechanical and electrical engineering and in the building industry. Alloys improved in strength and with a high corrosion resistance are used in aerospace, marine and engineering applications. Because of the low weight in relation to strength, aluminium is an interesting construction material. The density is almost three times less than for steel and its weight in a structure can therefore be drastically reduced by using aluminium alloys instead of for example stainless steels. Its low weight is the reason for its extensive use in airplane skeleton that consist of 75% aluminium. The good corrosion resistance properties and high strength to density ratio have made aluminium very useful also in the automotive industry.[5, 6] The industry has a demand to reduce the fuel consumption and for this to be achieved the vehicle weight needs to be reduced. The use of lightweight materials such as aluminium is one way to achieve an enhancement in the fuel economy.
Aluminium is often used for construction parts such as engine blocks, fuel rails, filler pipes and carburettors. The use of aluminium is increasing steadily and applications of the metal are expanded to areas of air conditioning, chassis and body structure to name a few.[3, 8] To enable the use of aluminium in this wide area of applications, disadvantageous properties such as its low elastic modulus and mechanical strength need to be improved. Without sacrificing the beneficial properties of aluminium and too improve these two areas, hundreds of different aluminium alloys have been produced. These wrought and casted aluminium alloys belong to eight series of families. Alloys in the same series share common properties and vary in composition, properties and uses compared to another series. It is therefore essential to know all criteria's for the application and to select the correct aluminium alloy for a given application. An aluminium alloy in one series could be suitable in one certain application while it in another could be catastrophically to use.[5, 6]

The main corrosion resistance of aluminium and its alloys stems from the passive oxide layer present on the surface, Al_2O_3. In formula (1) the reaction of oxide formation is showed. When this oxide layer is formed naturally it is only 3-4 nm thick but with anodisation techniques it is possible to form an oxide film of 5-30 µm.[5]

$$2Al + 3/2\ O_2 \rightarrow Al_2O_3 \qquad (1)$$

To find out during which circumstances aluminium is immune, forms the passive oxide layer or suffering of dissolution, a Pourbaix diagram can be studied. In Figure 1.1 the Pourbaix diagram for the aluminium and water system show that the area of passivity is at pH~4-8.5. However the Pourbaix diagram gives a good indication of the passive and immune area of aluminium but it is important to remember that the diagram refers to pure aluminium in an ideal liquid. If the environment is changed also the properties of the oxide film is changed. [5, 6, 9, 10]

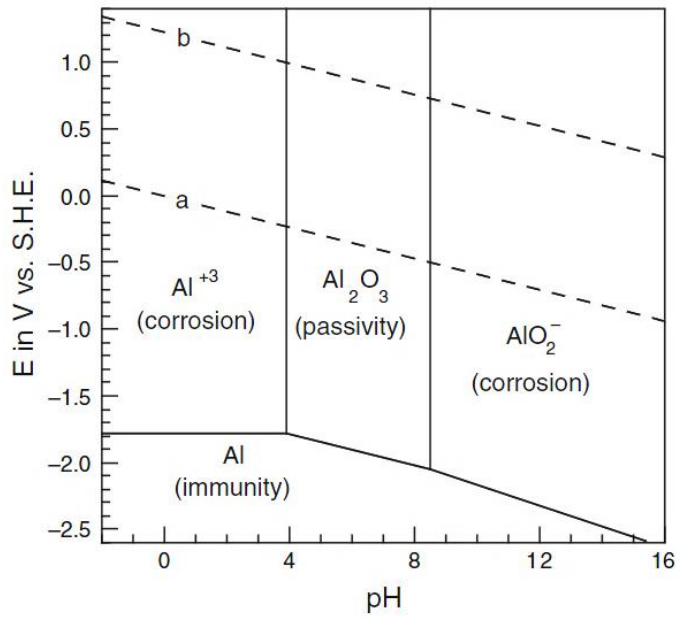

Figure 1.1. Pourbaix diagram of aluminium-water system. T=25°C, $a_{Al3+} = a_{AlO2-} = 10^{-6}$. The dotted lines show the domain of water stability.[9]

In the diagram also the simplified description of the aluminium species is shown; Al, Al^{3+}, Al_2O_3 and AlO_2^-. The species are in reality more complex and consist of solid species such as anhydrous oxide, Al_2O_3, hydroxides, $Al(OH)_3$, oxyhydroxides, AlO(OH), or soluble species as aluminium cations and anions. Of the anhydrous solid oxides consists only corundum which can be found in different rocks. The hydroxides have three variations; gibbsite, bayerite and nordstrandite. The stable phase of the aluminium species in contact with water or air is one of these hydroxides. Gibbsite occurs naturally in a mineral form and is produced in the extraction from bauxite. The oxyhydroxides have two variants which both naturally occur as minerals; boehmite and diaspora. These hydroxides can in aqueous solutions form gels, $Al(OH)_3 \times nH_2O$ ($n \geq 3$). These gels are unstable and amorphous with some traces of crystallinity. Upon aging they transform to gelatinous crystalline boehmite and eventually to bayerite.[5, 11]

1.3.2 Corrosion of aluminium

The electrochemical reaction of aluminium in aqueous medium results in the formation of trivalent cations Al^{3+} or hydroxide, $Al(OH)_3$. Corrosion of aluminium in aqueous medium cause an oxidation of the aluminium according to reaction formula (2):

$$Al \rightarrow Al^{3+} + 3e^- \quad (2)$$

Aluminium goes from oxidation state 0 to losing three electrons. This reaction is balanced by one of two reductions that can occur. Either the reduction of hydrogen, H^+:

$$3H^+ + 3e^- \rightarrow 3/2H_2 \quad (3)$$

Or the reduction of dissolved oxygen in:

- neutral or alkaline media: $O_2 + 2H_2O + 4e^- \rightarrow 4OH^-$ (4)
- acidic media: $O_2 + 4H^+ + 4e^- \rightarrow 2H_2O$ (5)

The result of the electrochemical reactions of oxidation and reduction is either:

$$Al + 3H^{+} \rightarrow Al^{3+} + 3/2H_2 \quad (6)$$

or

$$Al + 3\,H_2O \rightarrow Al(OH)_3 + 3/2H_2 \quad (7)$$

The aluminium hydroxide, $Al(OH)_3$, precipitates as a white gel and is insoluble in water. It is found in corrosion pits and appears as white gelatinous flakes and when dried it is present as bayerite. As can be seen in the reactions the corrosion development of aluminium causes a disproportionate volume of hydrogen compared to the amount of affected aluminium. This can cause severe accidents in closed areas.[5]

Different kinds of corrosion types can occur on aluminium. The most relevant types are briefly described in following sections.

1.3.2.1 Uniform corrosion

Uniform corrosion develops small pits in size of a micrometre over the entire sample surface. The thickness of the metal decrease after continued exposure. In environments of intermediate pH ~4-8 (see Figure 1.1) the oxide passive film protects the metal but in acidic and alkaline media, uniform corrosion commonly occurs. At these high and low pH levels the dissolution rate of the film is higher than the formation rate and the total dissolution rate can vary from a few micrometres a year up to a few micrometres per hour. The dissolution rate highly depends on the acid or base media properties. It has been observed that the dissolution rate is lower for long term- compared with short term exposures. Inhibitors, such as sodium silicate in alkaline media, can reduce the dissolution rate. By measuring the mass loss or the quantity of released hydrogen, the corrosion rate of uniform corrosion can be evaluated.[5, 9, 12]

1.3.2.2 Pitting corrosion

Pitting corrosion is a form of localised corrosion and the attack is located on a small area of the metal surface. The passive surface oxide suffers from a localised breakdown, often caused by chloride ions. The passive oxide film on aluminium alloys can also be disrupted by second-phase particles that can occur from the alloying elements.[5, 12] Pitting corrosion is a serious problem and on many materials it can take years to detect a pit. The pits can also initiate stress corrosion cracking in the presence of applied stress.[9]

Pitting corrosion is the most common form of corrosion for aluminium and the reaction is presented in reaction formula (8):[5, 10]

$$2Al + 3H_2O + 3/2O_2 \rightarrow 2Al(OH)_3 \quad (8)$$

Aluminium is susceptible to pitting corrosion in media of intermediate pH. This means that aluminium can be affected by pitting corrosion in almost all natural environments.[5] The solution within an initiated pit becomes acid and the pit will continue to propagate since the aluminium is not able to re-form the passive film.[10] When aqueous media is in permanent contact with aluminium, experience has shown that the pitting corrosion occur the first weeks of exposure. The corrosion pits are covered with the aluminium hydroxide gel, $Al(OH)_3$, which appears as gelatinous and white spots. In Figure 1.2 the corrosion mechanism of pitting corrosion is shown.[5]

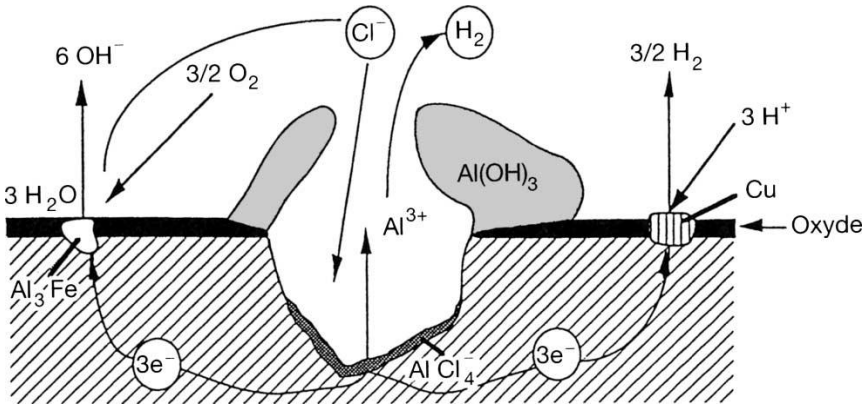

Figure 1.2. Schematic picture of pitting corrosion of aluminium.[5]

1.3.2.3 Filiform corrosion

Filiform corrosion is a corrosion mechanism that often occurs underneath a coating on aluminium, magnesium or steel. It can occur in humid conditions and is often initiated in a defect or a local damage in the coating. The corrosion appears as a narrow thread a few millimetres long and 0.1-0.5 millimetres wide. In Figure 1.3 the typical tracks of the active corrosion cell can be seen.

Figure 1.3. Filiform corrosion on painted aluminium.[13]

The corrosion cell consists of an active head (anodic site in front and cathodic site right behind) and an inert tail of corrosion products. See Figure 1.4 for an illustration of the corrosion cell.[13] The corrosion does not affect the mechanical properties and is most often mainly an aesthetic problem, but left untreated, the corrosion can cause more severe corrosion problems.[5, 12, 14, 15] For corrosion to propagate the presence of salts and oxygen is necessary. The presence of carbon dioxide, CO_2, has also been shown to enhance the risk of filiform corrosion on aluminium. Oxygen, or in some cases carbon dioxide, is supplied through cracks in the coating or through the corrosion products to the cathodic site in the active head. Filiform corrosion of aluminium usually occurs at a relative humidity between 75 and95% and at ambient or slightly elevated temperatures (20-40°C). In the presence of HCl-vapour, corrosion can occur already at a relative humidity of 30%.[12, 16]

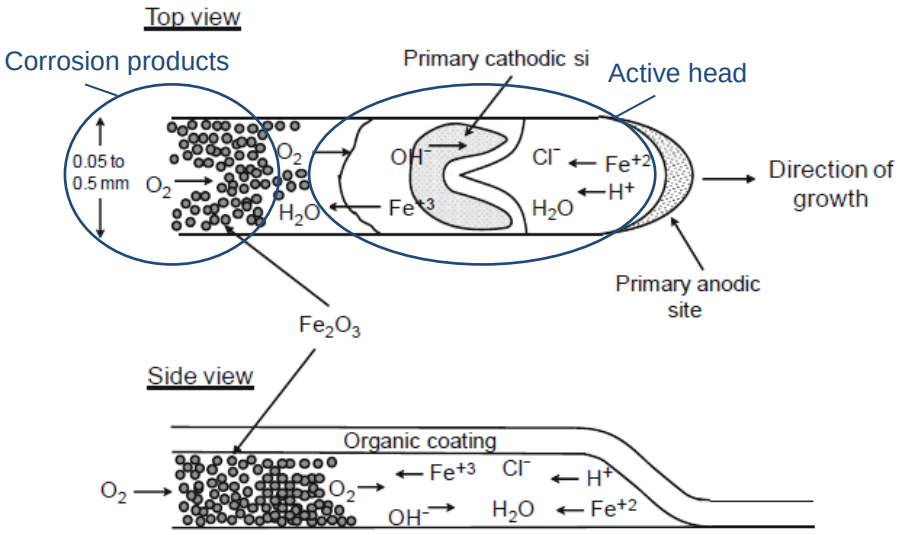

Figure 1.4 Illustration of filiform corrosion on steel.[9]

1.3.2.4 Galvanic corrosion

Galvanic corrosion is a corrosion mechanism that occurs when two materials of different nobility are in contact, mechanically or electrically. Corrosion occurs on the material with the lowest potential which due to this lower potential functions as an anode. The other, more noble, material functions as the cathode and remains relatively unharmed. Aluminium is one of the most electronegative materials (see Table 1.1) and this should mean that aluminium in contact with all materials above it in the standard electrode potential series would result in corrosion of aluminium. Experience has showed that this is not always the case since the passive surface oxide on aluminium provides good corrosion resistance in most applications.[5, 6, 9, 12]

Reaction	Potential (*V*)
$Au \leftrightarrows Au^{3+} + 3e^-$	+1.42
$Pt \leftrightarrows Pt^{2+} + 2e^-$	+1.20
$Pd \leftrightarrows Pd^{2+} + 2e^-$	+0.83
$Ag \leftrightarrows Ag^{2+} + 2e^-$	+0.80
$2Hg \leftrightarrows Hg_2^{2+} + 2e^-$	+0.80
$Cu \leftrightarrows Cu^{2+} + 2e^-$	+0.34
$H_2 \leftrightarrows 2H^+ + 2e^-$	0
$Pb \leftrightarrows Pb^{2+} + 2e^-$	−0.12
$Sn \leftrightarrows Sn^{2+} + 2e^-$	−0.14
$Ni \leftrightarrows Ni^{2+} + 2e^-$	−0.23
$Co \leftrightarrows Co^{2+} + 2e^-$	−0.27
$Cd \leftrightarrows Cd^{2+} + 2e^-$	−0.40
$Fe \leftrightarrows Fe^{2+} + 2e^-$	−0.44
$Cr \leftrightarrows Cr^{3+} + 3e^-$	−0.71
$Zn \leftrightarrows Zn^{2+} + 2e^-$	−0.76
$Ti \leftrightarrows Ti^{2+} + 2e^-$	−1.63
$Al \leftrightarrows Al^{3+} + 3e^-$	−1.66
$Mg \leftrightarrows Mg^{2+} + 2e^-$	−2.38
$Na \leftrightarrows Na^{+} + e^-$	−2.71

Table 1.1. Table of the standard electrode potentials.[5]

1.3.2.5 High temperature corrosion

The environments in high temperature corrosion can be quite different compared to environments for other corrosion types and it is of importance to be aware of the various influencing factors, such as temperature, time and gas composition.

Corrosion by reactions of an oxidising gas can occur at elevated temperatures without the presence of a liquid electrolyte. It can be called for example dry corrosion, gaseous corrosion or high temperature oxidation. The most common oxidising gas is oxygen, O_2, but also includes H_2O, SO_2, CO_2 and H_2S. This type of corrosion is usually connected to temperatures at several hundred degrees. Another form of corrosion at higher temperatures is hot corrosion that generally refers to the attack of salts or slags on the metal.[9, 12] At high temperatures and in dry atmospheres aluminium is relatively resistant to corrosion by most gases. However it is not resistant to halogens or their compounds. In aqueous systems aluminium can be affected of different corrosion attacks. At temperatures below 90°C the attack is usually in form of pitting corrosion. In range 90-250°C uniform corrosion is the most common form of corrosion and above 250°C aluminium is affected by intergranular attacks.[10]

1.3.2.6 Alcoholate corrosion

Alcoholate corrosion is a type of localised corrosion mechanism that can occur on aluminium, magnesium or lead[17] in alcohol blends, such as bio ethanol. The water content in the alcohol needs to be absent or very low for this corrosion to take place. Due to the low water content in bio ethanol, this type of corrosion phenomena is also called "dry corrosion".[5, 17-19] Figure 1.5 shows a corroded aluminium alloy AA6063 exposed to ethanol (E100) for 24 hours at 130°C. Almost the entire surface has been significantly corroded and in the figure the small circular holes typical for alcoholate corrosion can be observed.

Figure 1.5. Corroded aluminium alloy.

Alcoholate corrosion is a chemical reaction that proceeds very fast with H_2 gas development. The alcoholate corrosion involves three reactions. The first reaction (9) produces alcoholates, also called alkoxides or ethoxides, and these either becomes hydrolysed in reaction (10) or decomposed in reaction (11).[2, 5, 18, 19]

$$3C_2H_5OH + Al \rightarrow Al(C_2H_5O)_3 + 3/2H_2 \quad (9)$$

$$Al(C_2H_5O)_3 + 3H_2O \rightarrow Al(OH)_3 + 3C_2H_5OH \quad (10)$$

$$2Al(C_2H_5O)_3 \rightarrow Al_2O_3 + 6C_2H_4 + 3H_2O \quad (11)$$

So far this type of corrosion has not been sufficiently explained. The suggested corrosion process is that the passive surface oxide is damaged by attacks on mechanical flaws or cracks caused by an increased temperature or dehydration of the ethanol. In an environment of very low water content the passive surface oxide is not able to re-passivate and corrosion starts. Corrosion starts at weak points

and pits are formed. As can be expected from reaction (9), gas bubbles form and float up close to the pits. Both reaction (10) and (11) generate alkaline products and these accumulate in the pits or precipitate into solution. If the reaction products reach the critical level of pH 8 in aqueous solutions the passive surface oxide will break down. The mechanism will change to uniform corrosion and the corrosion process will accelerate.[19] To prevent alcoholate corrosion, as low water levels as 0.1% in bio-ethanols can be sufficient to enable the passive surface oxide to remain intact. [17]

1.3.3 Surface treatments

Surface treatments on metals are used to hinder the underlying metal from corrosion and also provide an aesthetic improvement.[6] The surface treatments of most relevance for this work are described in following sections.

1.3.3.1 Anodisation

Anodisation is a surface treatment that can significantly improve the corrosion properties of aluminium and some of its alloys. The benefits of anodisation are not only the improvement of corrosion resistance but also the aesthetic appearance, and improved adhesion of paint and other commercial applications. The anodised layer is an insulator, and unlike metallic coatings that are cathodic to the metal, a local breakdown will not accelerate a potential corrosion. The anodised layer can be as thick as 500 µm but is generally 5-30 µm thick. The layer is dense, hard, electrically insulating and wear resistant. Even though anodisation is a complex and complicated process it is an easy practiced technique and therefore frequently used.[5-7, 20-23]

Anodisation is a technique in which the surface of a metal is converted to a complex oxide ceramic layer. A metal in a suitable electrolyte, usually sulphuric or phosphoric acid, is applied to an anodic potential and a thick oxide film is formed on the metal (see Figure 1.6). The anodised film has a thin barrier layer closest to the surface. This layer is overlaid by a micro-porous layer which is sealed by post-anodising treatment resulting in an impermeable hard film.

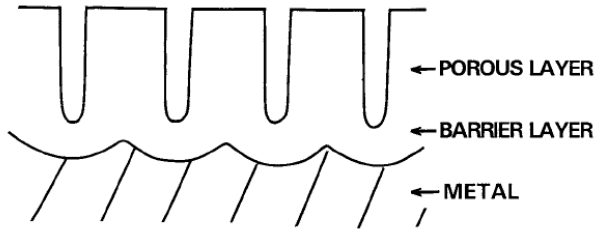

Figure 1.6. Illustration of anodised sample.[20]

The anodisation process operates at potentials above the breakdown potential and over the passivated metal surface, multiple arcs are moving rapidly with an oxide film growth as a consequence. Inside the growing layer is voltage breakthrough channels formed where complex compounds can be synthesised. The compounds consist of oxides from the metal and from elements of the electrolyte. Local temperatures can be very high but the temperature of the compounds does not become higher than 100°C. Specific combinations of current regime and electrolyte combination modifies the microstructures and phase composition of the metal providing a complex oxide ceramic layer.[6, 7, 20, 21]

The anodised layer contains pores and the electrolyte properties, temperature, anodising current density and voltage relate to the pore distribution and dimensions. Treatment during a longer time period results in a thicker layer and a thick oxide layer can act as a barrier of a high corrosion protection. Sealing of the open pores is usually performed after the anodisation process. Sealing increases the corrosion resistance and in some cases also the hardness and wear resistance. Before sealing, the film is porous, and corrosive ions can easily infiltrate the pores and attack the substrate. The anodised oxide film is usually sealed by treatment in hot water or steam with hydrated base metal species or treatment with sodium silicate.[6, 12, 21, 24, 25] In a hot water bath the film reacts and forms a crystalline hydroxide which is a form of pseudoboehmite, see reaction formula (12). The formation of pseudoboehmite results in a volume expansion and the pores are sealed.

$$Al_2O_3 + nH_2O \rightarrow Al_2O_3 \cdot nH_2O \qquad (n=1.5\text{-}2) \qquad (12)$$

Another way to seal the pores is by using cold sealing process. This process is performed at ambient temperatures and because of the low energy consumption it has become quite popular. It is performed in solutions of nickel and fluorine ions (Ni^{2+}, F^-) and the reaction (13) with aluminium oxide results in an aluminium-nickel-fluorine-complex that seals the pores.[12, 25]

$$Al_2O_3 + nNi^{2+} + xF^- + H_2O \rightarrow Al_2Ni_n + F_x(OH)_y + (6\text{-}y)OH^- \qquad (13)$$

1.3.3.2 Keronite coating

Keronite is a technology that originates from a space program in Russia and is now developed by Keronite International Ltd in the UK. The technology has showed good qualities in comparison with traditional methods, such as hard anodisation and nickel coating. Keronite is a plasma electrolytic oxidation (PEO) process in which a metal is placed in an electrolyte with a plasma discharge that converts the metallic surface into a complex ceramic oxide. The Keronite process is complex and involves different combinations of oxide growth, recrystallisation and partial metal dissolution. The metal surface is exposed to extensive plasma discharges and high local pressures but as the process is at microscopic levels no heat or distortion areas occur. The process can be performed at low temperatures in the range of 12- 30°C and the electrolyte is a low concentrated alkaline solution without any heavy metals and is non-hazardous. The Keronite coating has a high barrier capacity to hinder corrosion but before it can be more frequently used in the industry it need to become more cost effective.[21, 26, 27]

The coating consists of three different layers; a thin intermediate layer between the metal and the ceramic oxide, a dense middle layer of merged ceramic oxides and a top layer of? The middle layer is the main layer which provides the functional characteristics, such as wear resistance and hardness. The thickness of the top layer is 10-20% of the total thickness and is a porous layer on which a top coat easily can adhere.[21, 26, 27] During the growth of the coating different typical features can occur and these are shown in Figure 1.7. Localised discharges cause volcano-like eruptions to occur repeatedly and these results in the formation of craters (a). The centre of these craters has deep shrinkage holes (b) and from the craters, material is ejected in a globule form (c). In the coating localised micro-cracks (d) can be found and these are usually in a radial direction to the craters.[28]

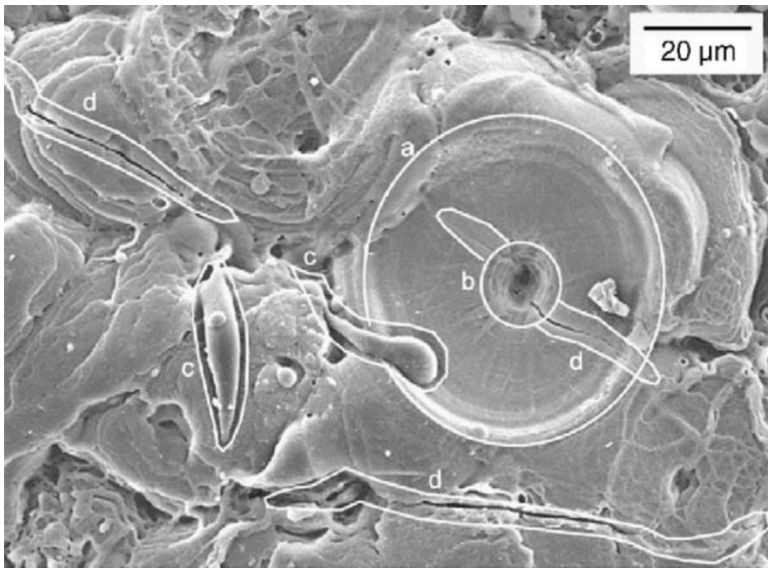

Figure 1.7. SEM micrograph of aluminium alloy BS Al-6082 with 40 µm thick Keronite coating. a) crater. b) shrinkage hole. c) ejected material. d) micro-cracks.[28]

The thickness of a Keronite coating is most often in the range between 10 and80 µm and the film is harder than other anodised surfaces. Different materials can be impregnated into the ceramic oxide to further improve the coating for corrosion and wear resistance. These materials can be different polymers, for example PTFE and organic polymers, or metals such as Cr or Ni or even ceramics via sol gel and PVD processes.[21, 26, 27]

1.3.3.3 Nickel coating

The nickel coating investigated in this study is electroless nickel plating with medium (6-9%) and high (10-13%) phosphor content. Nickel-phosphorous alloy coatings have shown good resistance to corrosion and wear, high hardness and paramagnetic properties.[29] An increased phosphorous content improves the resistance of corrosion for the coating in contact with bio diesel.[30] Other successful coatings have shown to involve the metals nickel, copper, platinum, gold, silver, cobalt and palladium or alloys including these metals.[29] The electroless coating have however showed poor corrosion resistance in chloride solutions.[31]

Products with electroless nickel-phosphor coatings are used in wide areas such as the automotive, offshore, mining and food industries. [32] The coating has great barrier qualities and can efficiently separate the material from the surrounding environment.[33] A great advantage with this coating compared to the electrolytic processes is the possibility to make a more even distribution on the surface.[32] A disadvantage with this coating is the risk of a local attack at a defect or surface damage and the possibility of an unfavourable small anode and large cathode that accelerates the corrosion process.[6] The porosity of the coatings is an important factor for corrosion to occur. Generally the corrosion resistance is increased by a thicker coating, which provides fewer pores that actually penetrate the coating.[34]

The electroless coating is achieved without electric current in a bath controlled in pH and temperature. The bath consists of the pre-treated substrate, reducing agent, complexing agent, bath stabiliser and aqueous solution of metal ions. The ions are usually nickel sulphate or nickel chloride when nickel is the depositing element of the coating. During controlled temperature the coating layer is formed when the metal ions is reduced and positioned onto the catalytic surface layer. The layer grows with one atom at a time, an even distribution of the deposited metal over the entire surface area.[29]

1.3.4 Ethanol

The interest of using biofuels is increasing for reasons related to environmental concern, sustainability, diversity and energy security. The ethanol biofuel is considered to be a good alternative fuel to gasoline. The commercial production of ethanol is either by conversion of ethylene or fermentation of biomass. Biomass is a renewable energy and the fermentation is often of corn but also other biological materials such as sugar, cellulose or starch can be used for ethanol production.[35, 36] The impact of replacing ethanol for gasoline provides both positive and negative results. Ethanol can manipulate the fuel oxygen level and enhance octane, but since gasoline has a higher vapour pressure than ethanol, ethanol fuel can result in cold start difficulties for engines. The compatibility between construction materials and alcohols has some concerns, such as metal corrosion and swelling of elastomers. An increased use of ethanol would raise the toxic emissions of acetaldehyde and PAN (Peroxyacytylnitrate) but reduce emissions of benzene, POM (Polyoxymethylene) and 1,3-butadiene. The greenhouse effect depends on how the energy source of the ethanol feedstock is assumed. The ethanol feedstock from cellulosic biomass gives for example much lower CO_2 burden than the corn feedstock.[37]

1.3.4.1 Ethanol and water

Ethanol is a hygroscopic liquid and the manufacture of an anhydrous ethanol is difficult. Ethanol and water forms an azeotropic mixture making it difficult to separate them.[38] An azeotrope is defined as a liquid mixture of components which together results in a lower or higher constant boiling point than that of each component (see Figure 1.8).

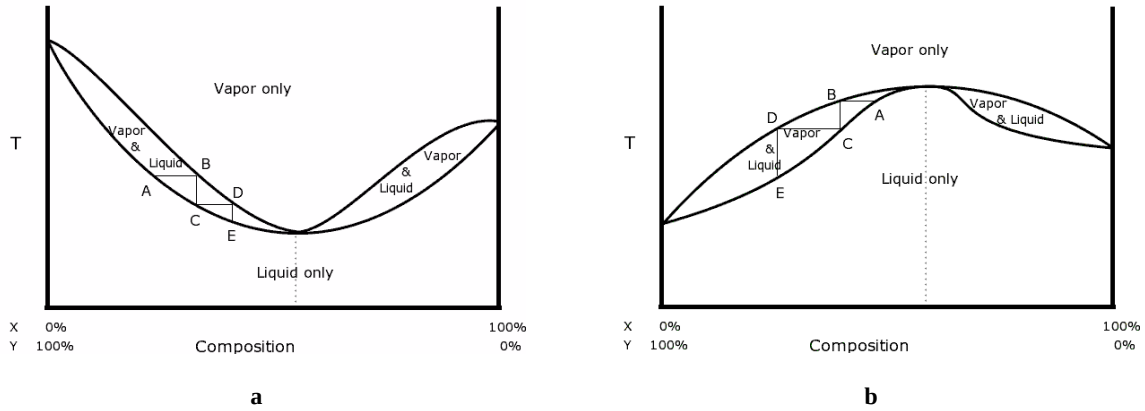

Figure 1.8.a) Positive azeotrope with lower constant boiling point. b) Negative azeotrope with higher constant boiling point.

A solution of ethanol and water creates a positive azeotrope and has a lower boiling point than the liquids separately.[39] At an atmospheric pressure of 1 bar, water has a boiling point of 100°C, ethanol 78.3°C. Combined, their boiling point is 78.174°C.[40] There exist some processes to separate ethanol and water, one is azeotropic distillation. This enables fluids to be separated to a certain extent but the process is very energy consuming.[38] Regardless of the azeotropic starting mixture of ethanol and water, a solution of 95.6% ethanol is possible via distillation.[39]

In Figure 1.9 the vapour and liquid equilibrium is shown for ethanol and water. With a starting liquid mixture of 0.2 mole fraction of ethanol (A) the vapour will consist of 0.53 mole fraction of ethanol (B). By using the resulting solution of 0.53 mole fraction and distil once more, it is possible to obtain approximately 0.68 mole fraction of ethanol.[41] This process is achievable to the azeotropic point at 0.956 mole fraction ethanol.[39] In a system with an ethanol and water blend where the ethanol

content is lower than 95.6% through heating, it will result in a vapour with higher ethanol content compared to the gas. This extraction from the liquid will consequently result in a remaining liquid with higher water content.

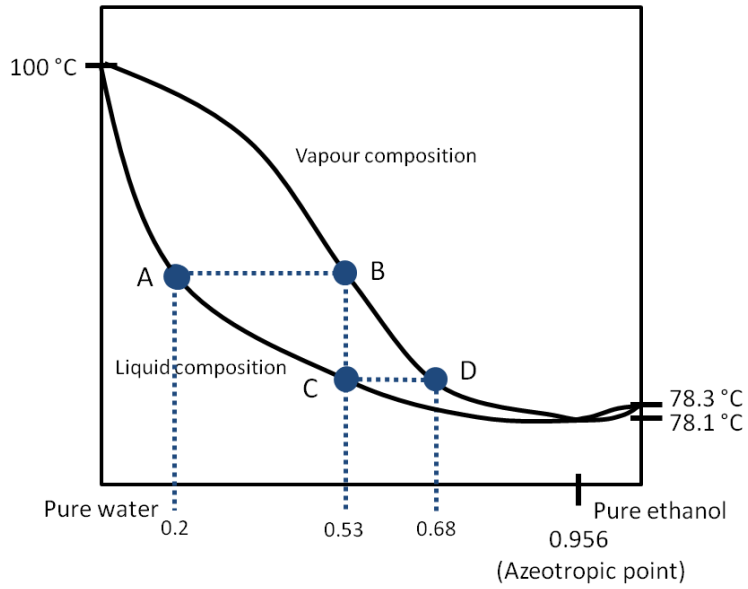

Figure 1.9. Vapour- liquid equilibrium of ethanol and water at 1 bar (figure is not to scale).

If the starting mixture of ethanol is higher than 95.6% the process will go in the opposite direction. Each distillation will go towards the azeotropic point at mole fraction 0.956, reducing the ethanol content in the distillate. In Figure 1.10 the starting mixture of ethanol (A) is above the azeotropic point. Consequently the distillation will go from the starting mixture A to mixture D. In a system with the ethanol and water liquid above the azeotropic point, heating the liquid will give a vapour of higher water content. The drainage of water from the liquid will give a higher ethanol percentage in the remaining liquid.

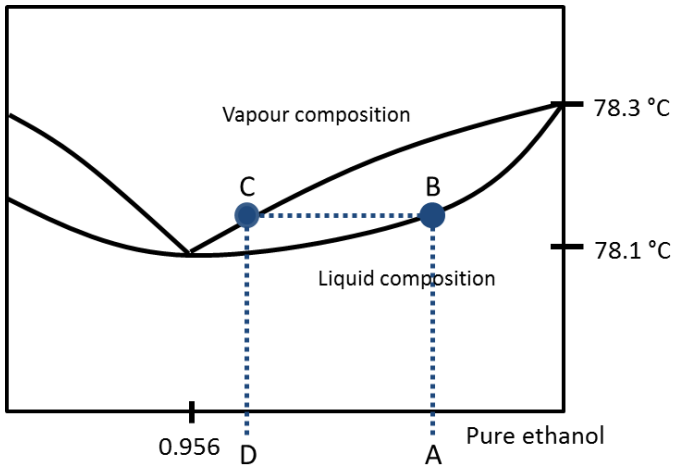

Figure 1.10 Vapour- liquid equilibrium of ethanol and water (figure is not to scale).

1.3.4.1.1 Temperature and pressure

By increasing the temperature more water content can be added to an alcohol solution without the occurrence of phase separation.[42] The literature also reveals that the equilibrium of the azeotrope of ethanol and water can be changed by means of changes in temperature and pressure. Barr-David and Dodge[41] have studied the ethanol and water system with isothermal process at 150, 200, 250, 275, 300, 325 and 350°C. These results are graphically shown in Figure 1.11-1.13. Figure 1.11 shows the azeotropic behaviour between water and ethanol at elevated temperatures and pressures. The increase of temperature and pressure moves the critical point (in the figure it is where the data crosses the critical locus) of the azeotropic behaviour to lower ethanol mole fractions. After the critical point, above the critical locus, the ethanol and water composition does not change between the liquid and vapour phase.[41]

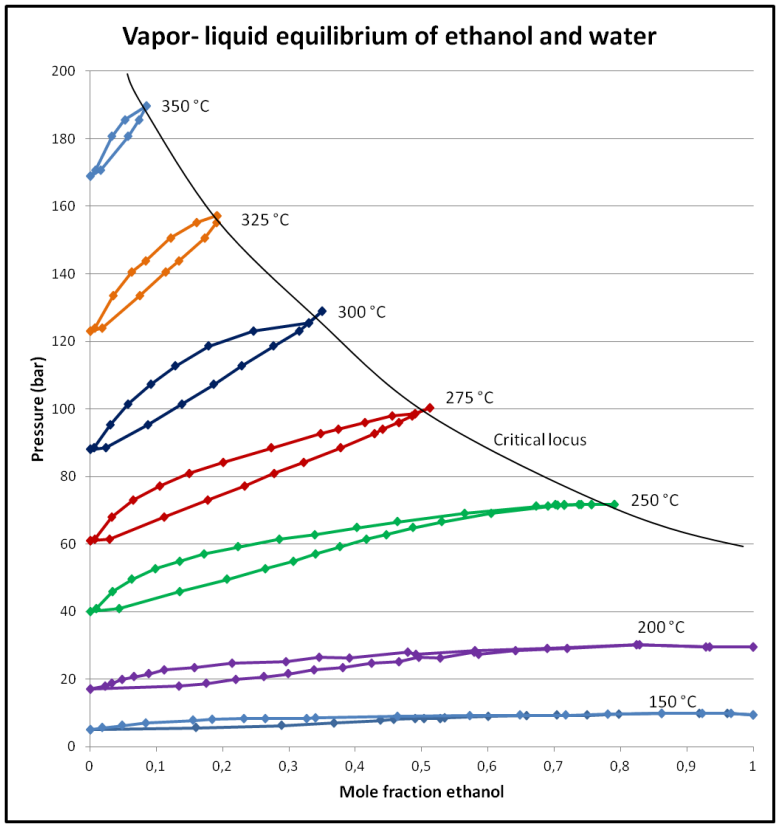

Figure 1.11. Ethanol composition at elevated temperature and pressures. Upper line is liquid and under line is vapour.[41]

Figure 1.12 shows that a liquid of 0.9 mole fraction ethanol at 250°C and at 70 bar has the same composition both in liquid and in vapour. An increase in temperature and pressure results in the possibility to have a solution of lower ethanol content without changing the composition between liquid and vapour phase. The azeotropic properties decrease with increasing temperature and pressure.

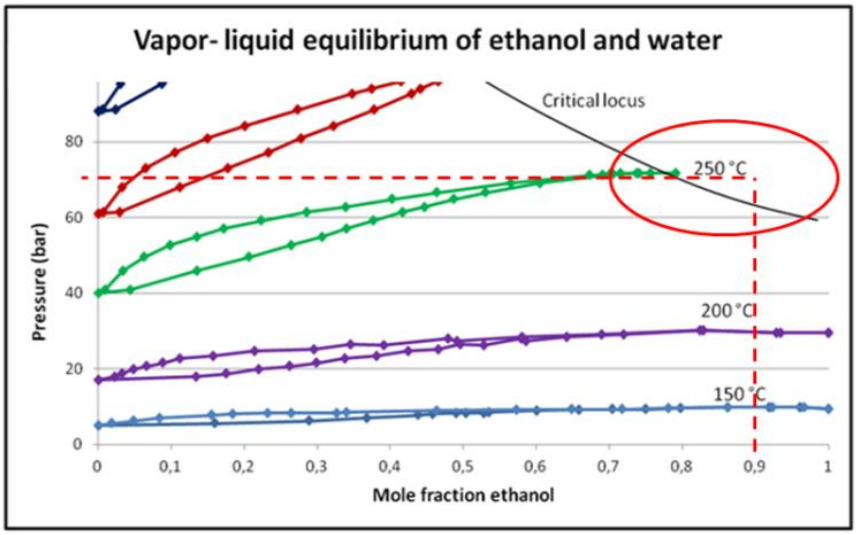

Figure 1.12. Equilibrium focused on 0.9% ethanol at 250°C and 70 bar (enlargement from Figure 1.11).

In Figure 1.13 the isotherms of ethanol and water is shown. The figure shows differences in composition between the liquid and the gas phase. When the temperature increases, the composition liquid and vapour becomes gradually more similar. In the region of >0.8 mole fraction ethanol, the lines of liquid and vapour become close and all of the isotherms have the similar composition in liquid as in vapour. It is uncertain if the azeotrope exists in ethanol and water solutions with >0.8 mole fraction ethanol at temperatures above 150°C.[41]

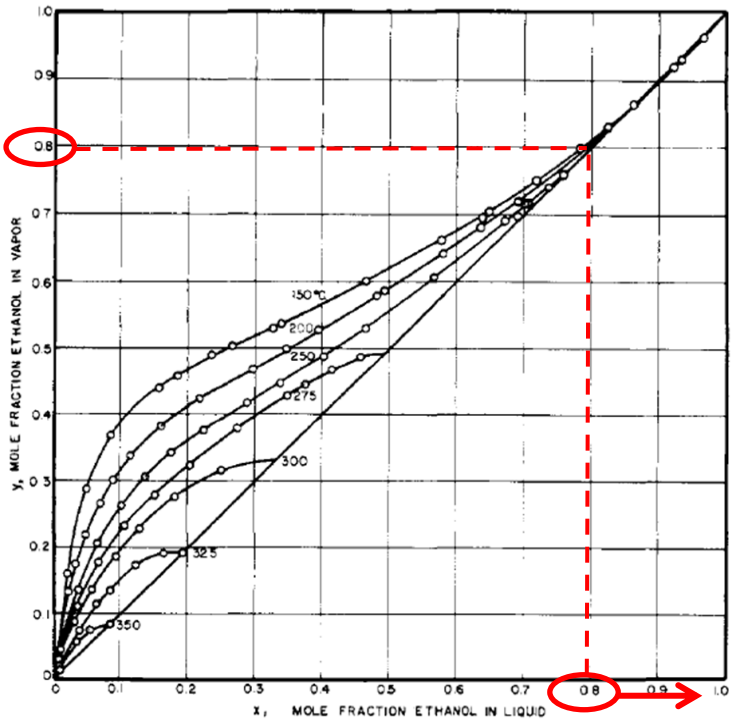

Figure 1.13. Isotherms of ethanol and water.[41]

Isobaric measurements accomplished by Barr-David and Dodge are presented in Figure 1.14. The experimental data of the isobars are of 1, 34, 69, 103, 138, 172 bar. At 1 bar (14.7 psia), a 0.2 mole fraction ethanol in liquid results in a 0.53 mole fraction ethanol in vapour. This results in a difference

of 0.33 mole fraction ethanol. At the pressure of 172 bar (2500 psia), 0.2 mole fraction ethanol is the same in both the liquid and the vapour. This indicates that a higher pressure results in a smaller difference between the composition in the liquid and the vapour.

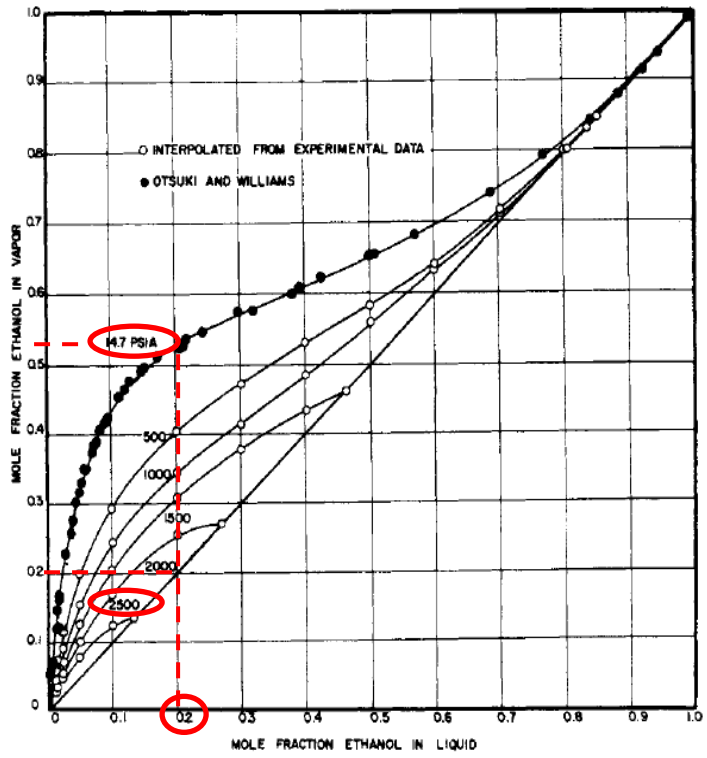

Figure 1.14. Isobars of ethanol and water.[41]

Evaluation of Figure 1.13 and Figure 1.14 shows similar results. It is apparent that the isotherms and isobars of ethanol and water follow the same trend. Higher temperature or pressure results in an increasingly constant composition of ethanol and water. In both cases of the isotherms and the isobars, and when the ethanol content is above 80%, the composition is the same in the liquid and the vapour phase. These results of Barr-David and Dodge have also been studied and verified in other studies.[43-48]

Pressurisation with oxygen or nitrogen on ethanol has showed that oxygen is many times more soluble in ethanol compared to nitrogen. This behaviour is independent of changes in temperature and pressure.[49] Ethanol and oxygen react according to equation (14) and form acetic acid and water:

$$C_2H_5OH + O_2 \rightarrow CH_3COOH + H_2O \text{ [19]} \quad (14)$$

1.3.4.2 Ethanol, water and gasoline

Ethanol added to gasoline changes the properties of the fuel, which can influence the performance in the engine. Depending on the engine capacity it can affect the emissions, fuel economy, durability and operability.[1] Additives, such as ethanol and MTBE (methyl-tertiary-butyl-ether) are used to oxygenate gasoline for the intention to reduce the carbon monoxides produced during burning of the fuel.[1, 50] The addition of ethanol in gasoline results in a higher oxygen content in the fuel and a higher amount of ethanol, which consequently will give a more oxygenated fuel.[1] Automotive fuels have to improve octane ratings to reduce the environmental concern related to emissions of carbon

monoxide and organic compounds. This has resulted in that oxygenated compounds have an important factor in the fuel formulation.[51]
Anhydrous ethanol and gasoline are completely miscible but small amounts of water can separate them to some extent. If the water content is high enough, the blend will separate to an upper phase with more gasoline and a lower phase with more ethanol and water.. The lower phase has a higher density and a larger volume than the upper phase. An increase of water will eventually result in a full separation of two phases.[35] A solution of E10 (10% ethanol, 90% gasoline) with a water content above 0.5% can result in phase separation.[17] When separation occurs depends on temperature, ethanol and gasoline content and characteristics of the gasoline.[35] Euro95 (95% gasoline and 5% ethanol) has been studied down to temperatures of -25 °C with an added ethanol composition at the azeotropic point with 95.6% ethanol and 4.4% water. As long as the gasoline concentration is at least 95% no phase separation occurs.[52] The solution of only gasoline and MTBE is also miscible and the solution can solve water, but smaller amounts. When the water limit is reached and no more water can be solved, only the water phase will separate from the solution.[50]

As mentioned, the liquid combination of ethanol, water and gasoline is not totally compatible. Depending on the composition of the liquids, phase precipitation can occur. A ternary phase diagram of the three fluids provides an understanding of where the solution is miscible or immiscible. A diagram for the temperatures -10, 20 and 60°C is presented in Figure 1.15.a. From the diagram it is possible to determine that an increase in temperature makes the three liquids more and more compatible and miscible with one another. A composition of very low water content, <2%, is presented in Figure 1.15.b). When ethanol is decreasing and the gasoline content is increasing the ternary phase diagram, Figure 1.15.b), can be used. It shows that in a blend with ~15% ethanol and ~85% gasoline, the solution is close to the miscible and immiscible zones. A liquid with low water levels should be miscible if the ethanol content is above 15%, and consequently the gasoline content less than 85%. An increase in temperature will result in the possibility for an increase in the gasoline content and subsequently a decrease in the ethanol content. With increasing temperature, the phase separation of the ethanol-gasoline solution decreases significantly. At approximately 60°C, the phase separation is practically absent.[53] It is important to be aware of that changes in the surrounding conditions, as an increase in the moisture content or a decrease in temperature, can cause spontaneous phase separation to occur.[42]

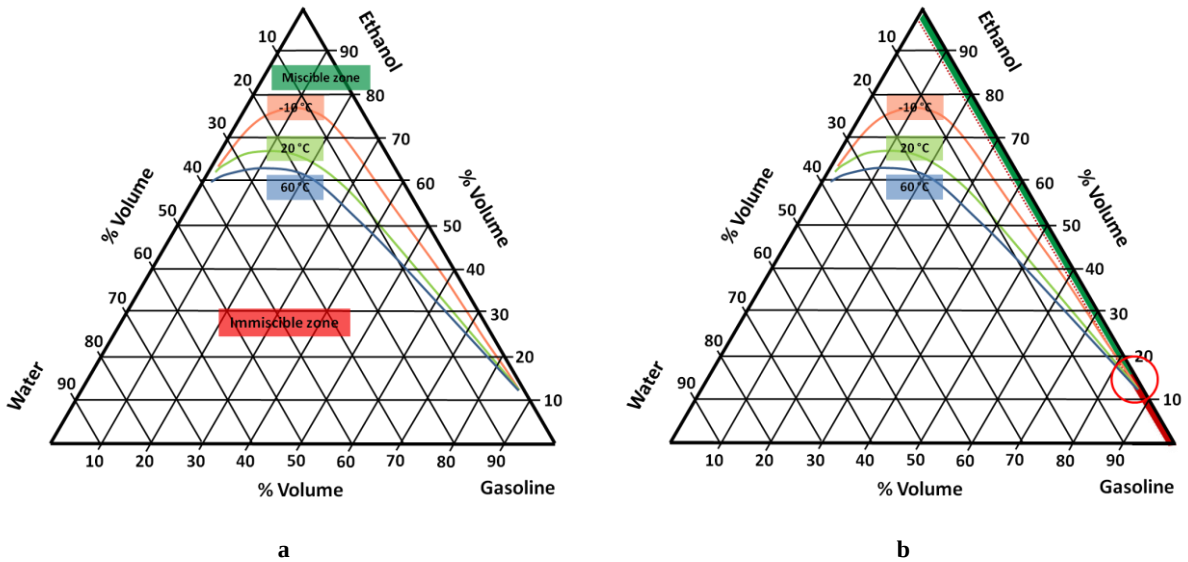

Figure 1.15.a) Phase separation of ethanol, water and gasoline at -10, 20 and 60°C. b) At low water content. Figure summarised and reconstructed from [46, 54].

1.3.5 Corrosion of aluminium in contact with ethanol

Corrosion of aluminium in contact with ethanol has been studied. Pitting and alcoholate corrosion have been shown to occur on aluminium and its alloys in contact with ethanol blends.[4, 17-19, 53] Focus in this study has been to determine predominating exposure parameters for alcoholate corrosion to occur.
For alcoholate corrosion an increased corrosiveness at higher temperatures and the correlation to chemical reactions have been observed.[19, 53] Since alcoholate corrosion is a chemical reaction it can be connected to the Arrhenius equation which describes the corrosion reaction rate coefficient and the fact that an increase in temperature results in an increased rate of chemical reactions:[5, 55]

$k=Aeexp(-E_a/RT)$

k= reaction rate constant
A= pre-exponential constant
E_a=activation energy
R=gas constant
T=temperature

Furthermore an acceleration of the alcoholate corrosion process has been noticed above the boiling point of the fuel solution.[19, 53] The lowest temperature when any attack has been observed is 60°C[19]. It has also been noticed that alcoholate corrosion occurs at a lower critical temperature in fuels of lower water content.[18, 19, 56] The time of exposure is also of great importance, a longer time of exposure can result in corrosion even at lower temperatures.[19]

Studies regarding to the electrolyte have showed an increased corrosiveness with increased ethanol content. A higher amount of ethanol results to corrosion after a shorter incubation time and at a more rapid rate.[19, 53] Comparisons of E25 (25% ethanol 75% gasoline), E50 (50% ethanol 50% gasoline) and E85 (85% ethanol 15% gasoline) have shown that E50 and E85 are more aggressive than E25. Krüger et al. explains this behaviour as a result of less corrosion products formed on samples in E25 when local corrosion turns into uniform corrosion. These corrosion products form a thick layer and reduce the corrosion rate. Their investigation also noticed that higher ethanol levels resulted in more rounded edges of formed pits and also in a larger number of corrosion pits.[19]

A study by Yoo et al. showed localised pitting corrosion on aluminium alloy A384 in E10(10% ethanol 90% gasoline) at 100°C.[53] This is of great interest as E10 is the recommended upper ethanol limit in fuels for ordinary motor vehicles.[1] The report recognises that another mechanism than pitting corrosion occurred on the corroded aluminium surface, see reaction (9).[53]

From a general corrosion perspective, the presence of water can be both beneficial and disadvantageous. The presence of water can cause electrochemical corrosions, such as wet or general corrosion while the lack of water can cause the chemical alcoholate corrosion.[17]

According to Vargel[5] the protective surface oxide of aluminium can be attacked by dehydrated alcohols at high temperatures resulting in the formation of an alcoholate, $Al(RO)_3$. Samples exposed to the vapour, or partially or completely immersed in alcohol, have all shown the same results, equation (15):

$$3ROH + Al \rightarrow 3/2H_2 + Al(RO)_3 \qquad (15)$$

$R=C_2H_5$ when ethanol is used

Vargel also considered the alcoholate to be soluble in the corrosive alcohol and not able to protect the aluminium surface with pitting corrosion as a consequence. The corrosion rate of aluminium in an alcoholic media depends on the temperature. Corrosion generally increases with temperature and no

significant effect occurs on aluminium at room temperature. A small amount of water will inhibit the corrosion process. Quantities as low as 0.05- 0.1% are sufficient for the protective natural oxide film of aluminium to form. Furthermore, the study states that ethanol or methanol in contact with aluminium cause similar corrosion behaviour. [5]

Eppel et al.[17] have studied alcoholate corrosion on aluminium alloys in contact with ethanol fuel blends. The test was carried out for five different aluminium alloys which were selected based on the criteria if they are commonly used in the automotive industry or not and if they have good corrosion properties. The alloys were exposed to almost water free E10 (10% ethanol 90% dry ASTM fuel C) in pressure proof vessels at elevated temperatures of 100, 110, 120 and 130 °C. Testing was performed according to the guidelines of the test standard VDA 230-207. If no corrosion occurred, the total test period lasted up to 168 h at each temperature. Results from this study indicate that the aluminium alloy composition does not have an influence on the risk of alcoholate corrosion above a temperature of 130°C. This report considers the ethanol content and the temperature to be the most important parameters governing alcoholate corrosion..[17]

Cast aluminium alloys were studied by Krüger et al., of which three were exposed without surface treatment and one with a chemically deposit nickel layer [ref]. The alloys were immersed for 336 hours in various ethanol fuel blends and water contents (0.05-0.3%) at temperatures ranging from room temperature to 80°C. The upper temperature of 80°C was chosen because this is estimated to be the highest temperature in fuel systems with low pressure. Alcoholate corrosion occurred at 60 °C and it was observed that the corrosion process was accelerated above the boiling point and that an increase of the ethanol content and temperature results in a higher risk for corrosion. The aluminium alloys with a nickel coating showed a very god resistance to corrosion. The study concludes that the alcoholate corrosion primarily depends on the water content and the temperature and secondarily on the ethanol content.[19]

Krüger et al.[19] conclude furthermore that the mechanisms of alcoholate corrosion are not sufficiently explained. Due to the lack of relevance in the past, few investigations have been focusing on this type of corrosion. Before 2008, the water content in alcohol fuels was 1% or more. However, since 2008, it has been required to keep the water content below 0.3% at the petrol pump. Since ethanol is hygroscopic, the water content will increase during storage. To keep the required water limit, alcohol fuels with water contents as low as 0.05% can be found. This concentration is well within the range to cause alcoholate corrosion. Krüger et al estimated the critical water level of the ethanol blends (E10, E25, E50 and E85) to approximately 0.2%. Krüger et al. were also uncertain if a solution below this level is temperature dependent. [19]

Today in the fairly novel field of alcoholate corrosion, main research activities appear to take place at the Technische Universität Darmstedt in Germany and in the Republic of Korea.

An earlier study performed at Swerea KIMAB by Annika Talus has looked into the water dependency of alcoholate corrosion. Results from that investigation are presented in Appendix I. In Figure 5.10 the results from the earlier work is merged with the results in this study.

2 Experimental equipment

To characterise the materials in the study different characterisation methods were used.

2.1 FTIR

An established analytical technique for characterisation of materials is the Fourier transform infrared (FTIR) spectroscopy. Different bonds between atoms or functional groups vibrate and rotate at specific frequencies. These characteristic frequencies are correlated to a chemical structure of the material.

In the FTIR an infrared beam is directed to an interferometer (see Figure 2.1) and a beam splitter split the beam in two. One of the beams is directed to a fixed mirror and the other to a movable mirror. The two beams are reflected by the mirrors and recombine at the beam splitter. The movable mirror is moved and this result in a change of the optical path length and when the two beams are recombined a phase difference in the recombined beam occur. The beam passes a sample and the resulting signal is measured by the detector. A Fourier transform is performed on the signal providing a spectrum of the investigated sample.[57]

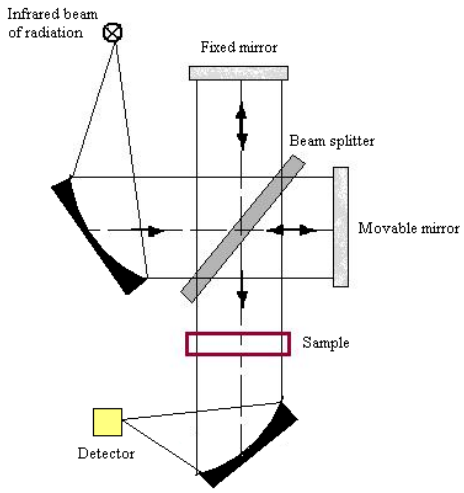

Figure 2.1. Schematic illustration of a Fourier transforms spectrometer.[57]

2.2 Polarisation measurements

Electrochemical polarisation is the shift in potential due to a flow of current from a change at an electrode. Polarisation measurements are used to acquire an electrochemical characterisation. With applied current on a sample the electrochemical corrosion rate can be calculated.[6, 12]

2.3 LOM

Light optical microscopy (LOM) is a commonly used characterisation method. The use of lenses and light on an area of the investigated sample engender an enlargement.

2.4 SEM

Comparable to LOM, the scanning electron microscope (SEM) magnifies the surface of an object. However, the magnification with SEM is significantly higher and can reach over 100 000x. Instead of light the SEM uses electrons to form an image. In Figure 2.2 an illustration of the SEM technique is shown. From the electron gun an electron beam is focused by travelling through electromagnetic fields and lenses before the beam hits the object. From the object electrons and X-rays are ejected and collected from detectors which convert them to signals for final image to be produced.[58]

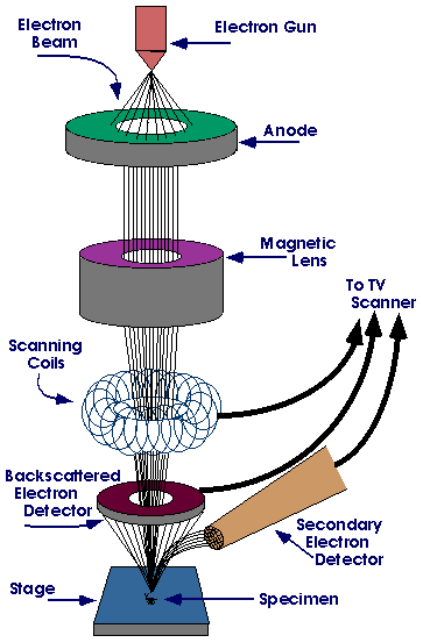

Figure 2.2. Illustration of SEM.[59]

2.5 Karl Fischer Coulometer

Karl Fischer Coulometer (Figure 2.3) is a titration technique used to determine the water percentage of a solution. The technique uses the reaction of iodine with water to calculate the amount of water present in a solution.[60] In this project an oven was also used.

Figure 2.3. Karl Fischer Coulometer with sample holder.[61]

3 Materials

3.1 Metals

The materials used in this study were mainly extruded aluminium alloy AA6063 but also the cast aluminium alloy A380 was used in a few trials. The size of the standard sample used was 100x25 mm. In Table 3.1 the composition of aluminium alloy AA6063 and A380 is shown. The analysis was performed by OES (optical emissions spectrometry).

Material	Si	Fe	Cu	Mn	Mg	Ni	Cr	Zn	Sn	Ti	Pb	Sr	P
AA6063	0.42	0.19	<0.01	0.04	0.46	<0.01	<0.01	<0.01		0.01			
A380	9.9	0.97	2.8	0.25	0.33	0.03		0.69	0.01	0.03	0.02	<0.01	<0.01

Table 3.1. Composition in wt-% of AA6063 and A380.

In one part of the study, different surface treatments on AA6063 were exposed to study the effect of the surface treatments upon alcoholate corrosion. The five surface treatments were:

- Anodisation with cold sealing, using nickel, thickness ~10 µm
- Anodisation with warm sealing in water, thickness ~10 µm
- Keronite coating, thickness ~20 µm
- Nickel coating (electroless nickel plating) with medium (6-9%) phosphor content, thickness ~10 µm
- Nickel coating (electroless nickel plating) with (10-13%) phosphor content, thickness ~10 µm

The cold sealing with nickel for the anodised samples was performed in a solution of PS41 (a solution from Metachem and known to contain nickel-fluorine and surface active elements). Sealing was executed in a bath of 140-160 g/L PS41 (corresponding to ~10 g/L nickel-fluorine) at the temperature 28-32°C, pH 5.8-6.4 and at 0.8-1.2 min/µm finishing with a short warm sealing of 0.5 min/µm. This process resulted in a sealing time of 1.3-1.7 min/µm.

Almeco Seal SLX from Almetron was the warm seal additive used for the other anodised samples. The content of this additive is not known but it contains most likely surface active elements that prevent the oxide to be overly sealed. The sealing treatment was performed in a bath of warm water with 2 g/L Almeco Seal SLX at 97°C, pH 5.8 which resulted in a sealing time of 3 min/µm.[62]

3.2 Fuels

Water free ethanol from Solveco of analytical grade 99.5% and unleaded gasoline from Statoil with Research Octane Number (RON) 98 containing MTBE were used.

4 Experimental procedure

4.1 Characterisation of materials

The different materials used in the study was characterised in order to establish corrosion and morphological characteristics of the surfaces and the outer surface oxide. This was made to be able to connect possible variations in the results to the different conditions of the materials. The methods used for this characterisation were LOM, SEM and polarisation measurements. Settings for the different tests are described in detail in following sections.

4.1.1 LOM

Cross sections of the AA6063 samples, with and without surface treatment were studied. The samples were prepared polished and the final step was with 1µm diamond paste. LOM pictures were collected with the magnification of 50-1000x.

4.1.2 SEM

The surface of the unexposed samples were studied with SEM. Pictures were taken on AA6063 samples and surface treated AA6063 samples with a magnification range of 25-10 000 x.

4.1.3 Polarisation measurements

Samples of the uncoated aluminium alloy AA6063 and the five surface treated AA6063 were exposed to polarisation measurements. The measurements are performed with Solartron Analytical, 1286 Electrochemical Interface. A silver chloride reference electrode with filling solution of saturated potassium chloride was used. The electrolyte consisted of 0.5 molar sodium sulphate and the exposure time was 40 minutes.

4.2 Ethanol exposure

4.2.1 Test method

Based on the literature investigation, the main parameters of alcoholate corrosion are water content, temperature, pressure and time. To evaluate how each parameter influences alcoholate corrosion, tests were performed using these parameters. By using autoclaves for the tests, a closed system was provided and the parameters before and after testing were controlled. In an autoclave (Figure 4.1a) the samples were exposed to ethanol solutions. Two samples of AA6063 or one sample of A380 were positioned into the autoclave and 120 mL ethanol solution was added (Figure 4.1b). The autoclaves were assembled with gaskets to prevent leakage.

a b

Figure 4.1.a) Disassembled autoclave. b) Autoclave with two samples of AA6063 in ethanol solution.

The autoclaves were placed in an explosion proof climate chamber, where they were heated to the test temperature. An explosion proof climate chamber (see Figure 4.2) is a safety chamber for hazardous products. Tests in the chamber can be both short and long term at temperatures up to 160°C. The reason why the autoclaves were positioned in the explosion proof climate chamber during the test was the risk of explosion when handling the fuels. Also the strong formation of hydrogen gas during the alcoholate corrosion process justifies using this equipment.

Figure 4.2. Picture of climate chamber.[63]

The autoclave tests in the explosion proof climate chamber were performed in two ways. In some tests the temperature and exposure times were varied manually.

Test time procedure a: The tests started from room temperature and the temperature increased to the selected temperature as fast as the capacity of the climate chamber (<0.5 h) allowed. The temperature was kept constant a selected time period and then cooled down for a time period of two hours to room temperature.

Test time procedure b: In the tests, the VDA 230-207 standard was followed. In Figure 4.3 the time and temperature profile of VDA 230-207 is shown. The testing started from room temperature and the temperature increased to 130°C for maximum five hours. The temperature was kept constant during

100 hours and within 15 hours it was cooled to room temperature. The samples were then stored at room temperature for maximum 48 hours before next test cycle.

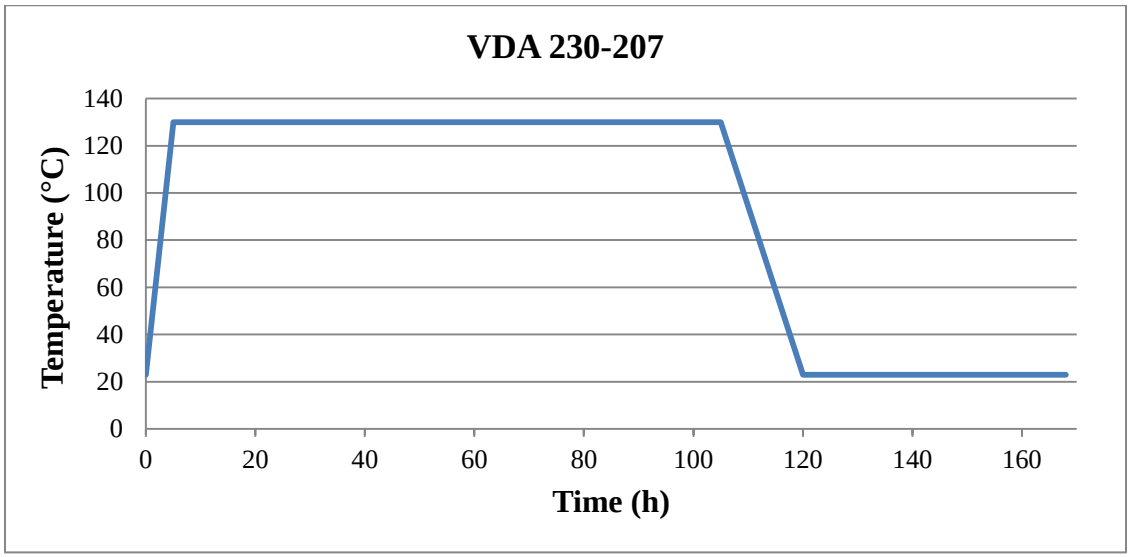

Figure 4.3. The standard test method VDA 230-207.

4.2.2 Water dependence

4.2.2.1 Different fuel blends

The water limit for alcoholate corrosion of different ethanol fuel blends has been explored. Samples of AA6063 were exposed to the blends which consisted of ethanol and gasoline mixed together from the composition E10 to E100. Small quantities of water were added into the solutions to find the water limits. The amount of added water was based on one trial to the next in order to find the water limits for alcoholate corrosion. When the autoclaves were prepared they were placed in the temperature chamber using the standard test method VDA 230-207. The solutions and the range of the tested water content is summarised in Table 4.1.

Solution	Ethanol (%)	Gasoline (%)	Water content (%)
E100	100	0	0.055-1.81
E85	85	15	0.08-1.15
E70	70	30	0.12-0.35
E50	50	50	0.18-0.36
E22	22	78	0.06-0.27
E10	10	90	0.05

Table 4.1. The solutions and range of water content used.

The water level before and after testing was also calculated for some of the tests in E85 and E100.

4.2.2.2 Liquid and gas phase

Testing was in addition performed in contact with liquid or gas to explore differences in the risk of alcoholate corrosion. The samples only exposed to the gas were placed above the liquid and sized to 25x25 mm. E100 and samples of both aluminium alloys AA6063 and A380 were used. For a complete list of the testing see Appendix II.

4.2.3 Surface treatments

Samples of the aluminium alloy AA6063 with and without surface treatments, described in part 3, were exposed in ethanol solutions of E85 (85% ethanol and 15% gasoline) in order to compare their corrosion behaviour. Two autoclaves with each material were exposed in parallel. To study the influence of water content in the ethanol solution, four different water contents in range of 0.18-0.48% were used, see Table 4.2. The tests were carried out with using the described test method VDA 230-207.

Test	Water content (%)
1	0.48
2	0.26
3	0.18
4	0.19

Table 4.2. Water contents in the E85-solution for the different tests.

4.2.4 Temperature

The aluminium alloy AA6063 was tested in autoclaves at different temperatures to explore how the temperature influenced alcoholate corrosion. The tested temperatures were in the range of 100-150°C (see Table 4.3). E100 was used and the water content level was attempted to keep constant in all tests to minimise this factor influencing the result. The water content was in the range 0.13-0.18% with two exceptions of 0.24% and 0.25%.

Temperature (°C)	100	120	125	125	130	135	140	145	150
Water content (%)	0.18	0.16	0.18	0.25	0.14	0.17	0.18	0.17	0.24

Table 4.3. Summary of the temperatures and water contents addressed in this study.

4.2.5 Time

A time dependency test for two specific temperatures was performed, 130 °C and 150 °C. The aim with this trial was to study the time for alcoholate corrosion to start. A logger was used to follow changes in the pressure in the autoclaves as an increase in pressure indicates initiation of alcoholate corrosion. The aluminium alloy AA6063 was exposed in E100 with a water content of 0.13%.

4.2.6 Pressure

To understand how the pressure influenced alcoholate corrosion, two pressurisation experiments were performed with aluminium alloy AA6063. In the main experiment oxygen, O_2, was used to pressurise the autoclaves. In the other secondary pressurisation test nitrogen, N_2, was used. Autoclaves with two aluminium alloy samples were filled with ethanol (E100) and pressurised with gas. In order to compare different pressures, each setup consisted of three autoclaves. The first was without any added pressure at the atmospheric pressure of 1 bar and the other autoclaves were pressurised with gas to 6 and 11 bar (see Figure 4.4). The exposure tests were performed with constant temperatures to separate the different pressures. The water content of the ethanol liquid was attempted to keep as low as possible and the water contents after exposure were analysed. The tests with samples in contact with the gas and the liquid consisted of samples with the standard size of 100x25 mm.

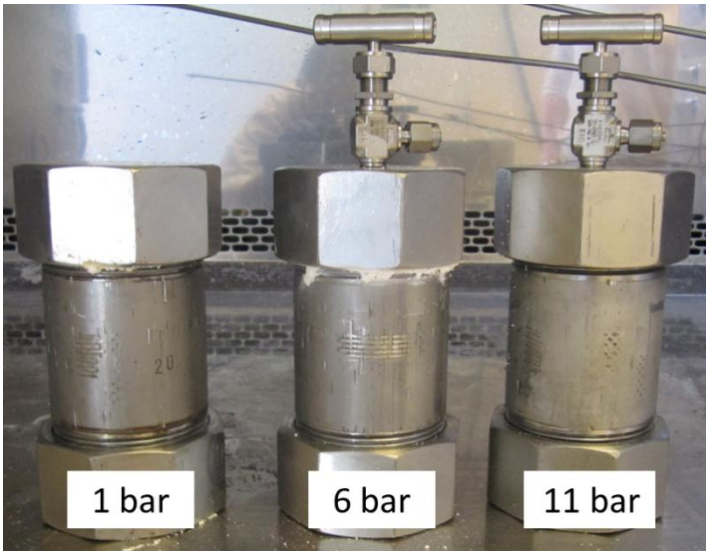

Figure 4.4. One setup consisting of three autoclaves with initial pressure of 1, 6 and 11 bar.

4.2.6.1 Oxygen

In Table 4.4 the pressurisation test with oxygen using samples of aluminium alloy AA6063 is presented. The time of exposure varied because the test was exploring the time until corrosion.

Test	Temperature (°C)	Time (h)	Water content (%)	Number of setups
1	120	96	0.16	3
2	130	24	0.14	3
3	150	12	0.24	3
4	125	36	0.18	3
5	140	24	0.18	3
6	125	72	0.25	1
7	135	54	0.17	3
8	145	18	0.17	1

Table 4.4. The pressurisation tests with oxygen using samples of AA6063.

4.2.6.2 Nitrogen

The second pressurisation test was performed with nitrogen and is presented in Table 4.5. AA6063 samples were placed in contact with gas and liquid. The exposure times varied because of the abrupt occurrence of corrosion.

Test	Temperature (°C)	Time (h)	Water content (%)	Number of setups
9	100	24	0.3	1
10	100	72	-	1
11	100	72	0.3	1
12	120	36	0.06	1
13	120	36	0.32	1
14	130	12	0.27	1
15	130	24	0.3	1

Table 4.5. Pressurisation test with nitrogen using samples of AA6063.

4.3 Characterisation of corrosion products

FTIR was used to characterise corrosion products of alcoholate corrosion from AA6063 samples. Dried and gel-like corrosion product samples were analysed and compared to the spectrum of ethanol and aluminium alcoholate. The aim with this study was to find the aluminium alcoholate and in that way prove that the reaction (9) of alcoholate corrosion had taken place. The other two reactions; (10) and (11), were also studied but were not the main purpose of this study.

5 Summary of results

The aim with the tests has been to get an overview of the areas of interest in connection to alcoholate corrosion. The experimental tests have in consequence focused on exploring all the different areas and not focusing on the generation of all tests necessary to get statistical reliability.

5.1 Characterisation of materials

5.1.1 LOM and SEM

In Figure 5.1 a sample of AA6063 is shown. In a) the even surface without coating can be seen and in b) the die lines from the production with extrusion of the aluminium alloy are shown.

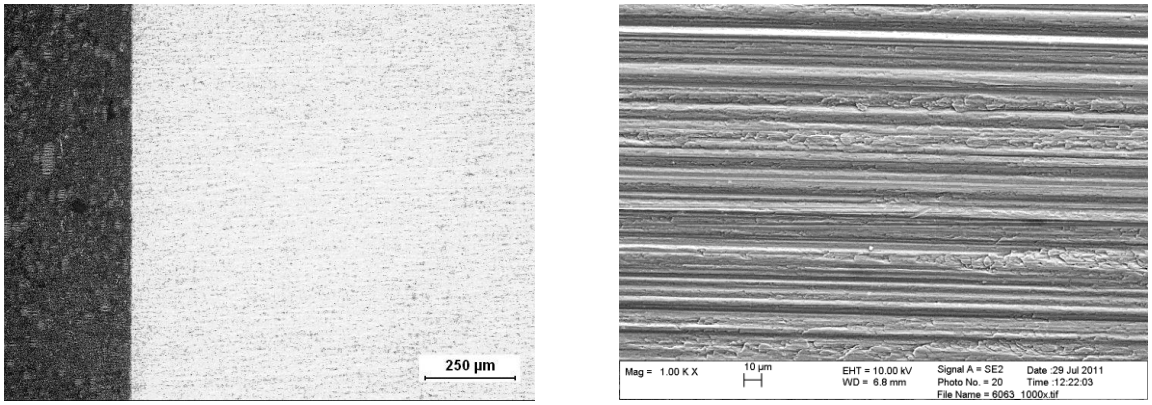

A **b**

Figure 5.1. Aluminium alloy AA6063. a) Cross section. b) SEM-picture with 1 000x magnification.

The anodised coatings are presented in Figure 5.2, cold sealed samples with nickel (a) and warm sealed samples in hot water (b). The coatings both showed a thickness of approximately 12 µm and were fairly evenly distributed on the aluminium alloy surface.

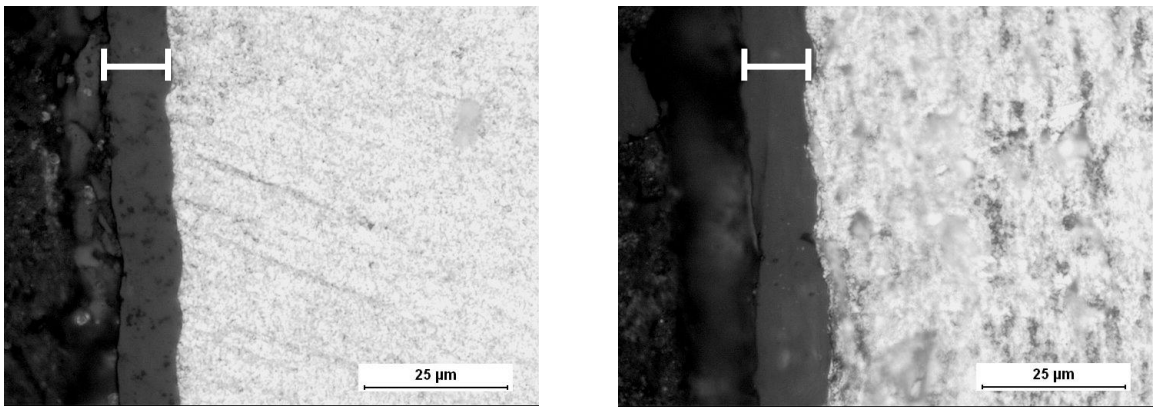

A **b**

Figure 5.2. Anodised coatings on AA6063. a) Cold sealed with nickel. b) Warm sealed with water.

Figure 5.3 show anodised AA6063 with a 1 000x magnification where a) is a cold sealed sample with nickel and b) is a warm sealed sample. In the SEM-picture the sealed pores from the anodisation and sealing can be seen.

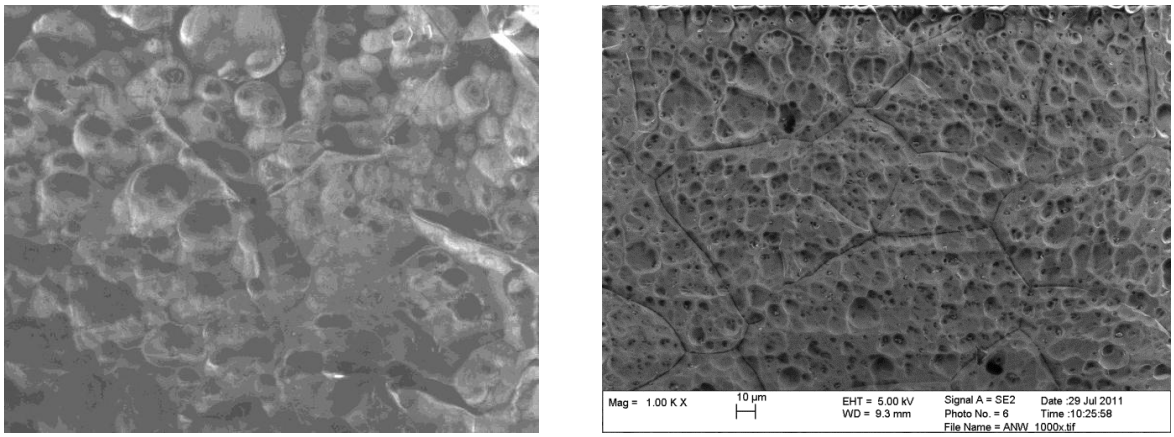

A **b**

Figure 5.3. Anodised AA6063. a) Cold sealed with nickel. b) Warm sealed with water.

Figure 5.4 show the Keronite coating. In a) it can be seen that the surface protection thickness vary from ~15 to 25 µm. The surface appears to be uneven and in the picture a pore from the production process is seen. In b) the pores and open holes can be seen.

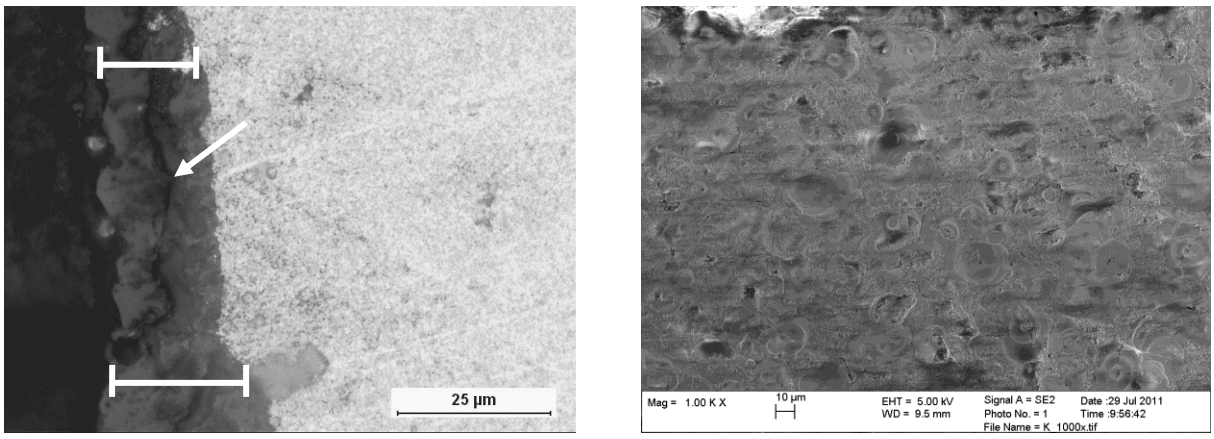

A **b**

Figure 5.4. Keronite coating on AA6063. a) Cross section. b) SEM-picture with 1 000x magnification.

Figure 5.5 shows cross sections of the nickel coatings. The coating with high phosphor content (b) has twice as thick coating compared with the coating with medium phosphor content (a). The thickness of the coating with high phosphor content is ~25 µm and the surface seemed a bit uneven. The medium phosphor content coating thickness is ~12 µm and the surface was more even. No defects on the surface can be seen in Figure 5.5 or the SEM-pictures in Figure 5.6.

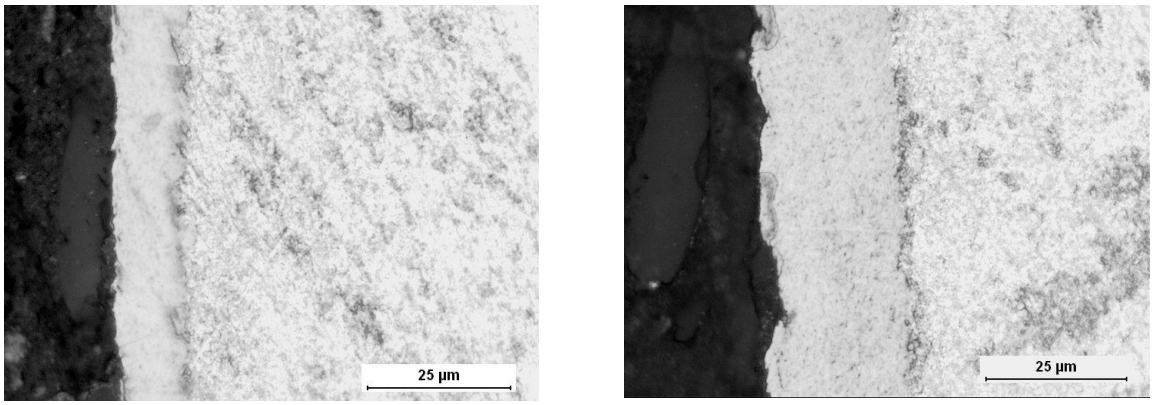

A **b**

Figure 5.5. Nickel coatings on AA6063. a) Medium phosphor content. b) High phosphor content.

The nickel coatings with medium and high phosphor content are presented in Figure 5.6 in 5 000x magnification. The coating with high phosphor content has larger nodular shapes compared with the medium phosphor coating.

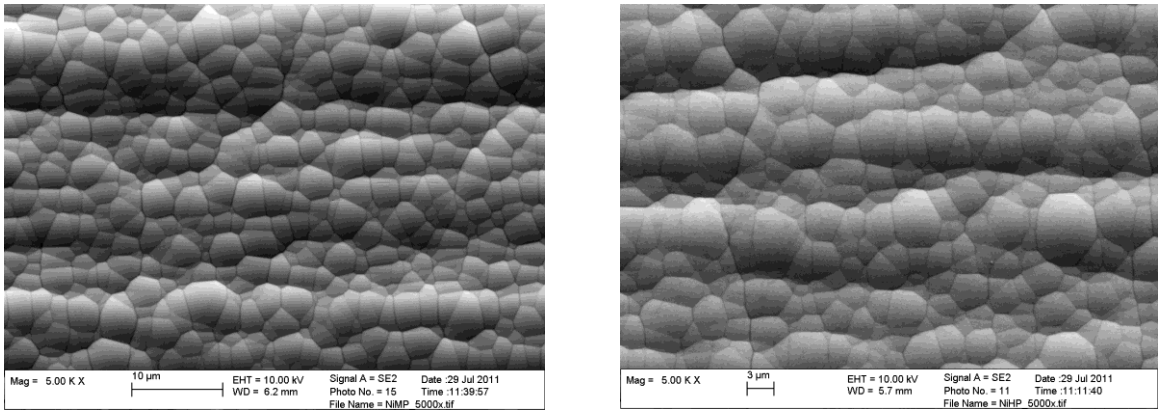

A **b**

Figure 5.6. SEM-pictures of nickel coatings on AA6063. a) Medium phosphor content b) High phosphor content.

5.1.2 Polarisation measurements

In Figure 5.7 the results from the polarisation measurements are presented. The results show that the surface treated nickel coatings electrochemically work as barriers against corrosion. The AA6063 coating forms a natural passive layer. The straight lines of the Keronite and the anodised coatings indicate that they are passive and that they are isolating coatings.

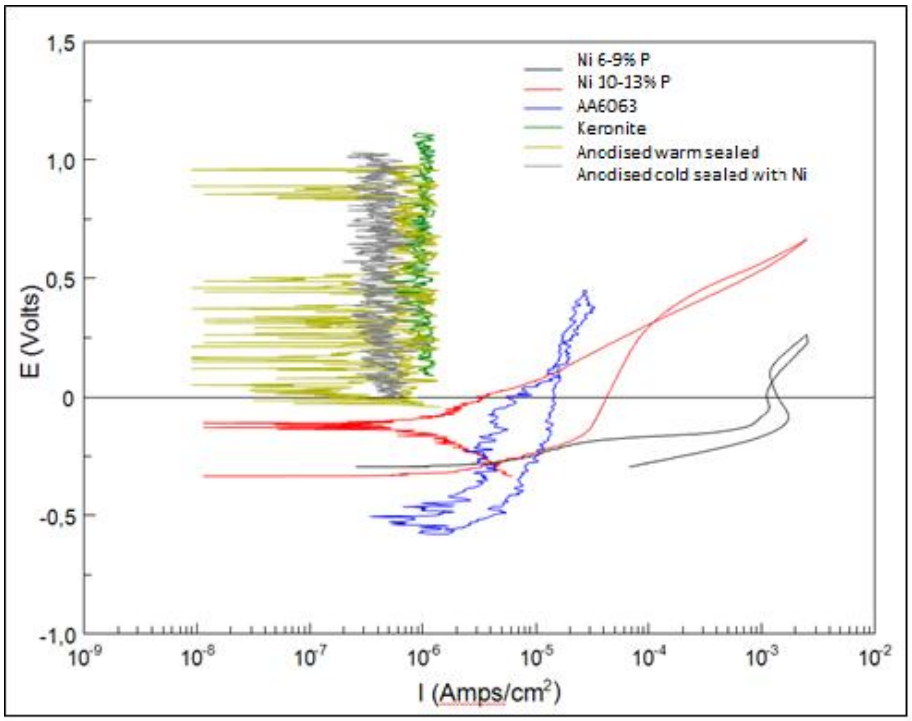

Figure 5.7. Polarisation measurement with AA6063 and surface treated AA6063.

In Table 5.1the results from the open circuit potential are shown. It shows that the uncoated AA6063 samples have a more negative potential compared with the other surface treated samples. The surface treated AA6063 was more noble compared with AA6063 samples.

Sample	E (V)
AA6063	-0.52
Anodised cold sealed with nickel	-0.21
Anodised warm sealed	-0.20
Keronite coating	-0.27
Nickel coating with medium phosphor content	-0.31
Nickel coating with high phosphor content	-0.34

Table 5.1. The open circuit potentials (vs. Ag/AgCl) of the uncoated AA6063 and the surface treated AA6063.

5.2 Ethanol exposure

5.2.1 Water dependence

5.2.1.1 Different fuel blends

In Figure 5.8 the results from the water limit test is shown. The figure illustrates if alcoholate corrosion has occurred or not for the different water contents in the ethanol blends. Each data point presents an autoclave. The red triangles represent autoclaves in which alcoholate corrosion has taken place and the green squares autoclaves where alcoholate corrosion has not occurred. The water limit that gives a risk of alcoholate corrosion needs to be observed as a risk area more than a given limit. There is no absolute limit between a safe and a no safe zone. There is an area where there is a higher risk of corrosion. The area of red triangles closest to no water content can be seen as a high risk zone. The area between the red and green points can be seen as an area where the risk of alcoholate corrosion to occur is high and above this area there is a low risk during these conditions.

The figure shows that alcoholate corrosion occurs within the range of approximately 0-0.4% water content with one exception at 0.82% in E85. Examination of Figure 5.8 also shows that an increase of the ethanol content up to E85 will lead to a wider high risk area. For E100 the risk area of corrosion is reduced again.

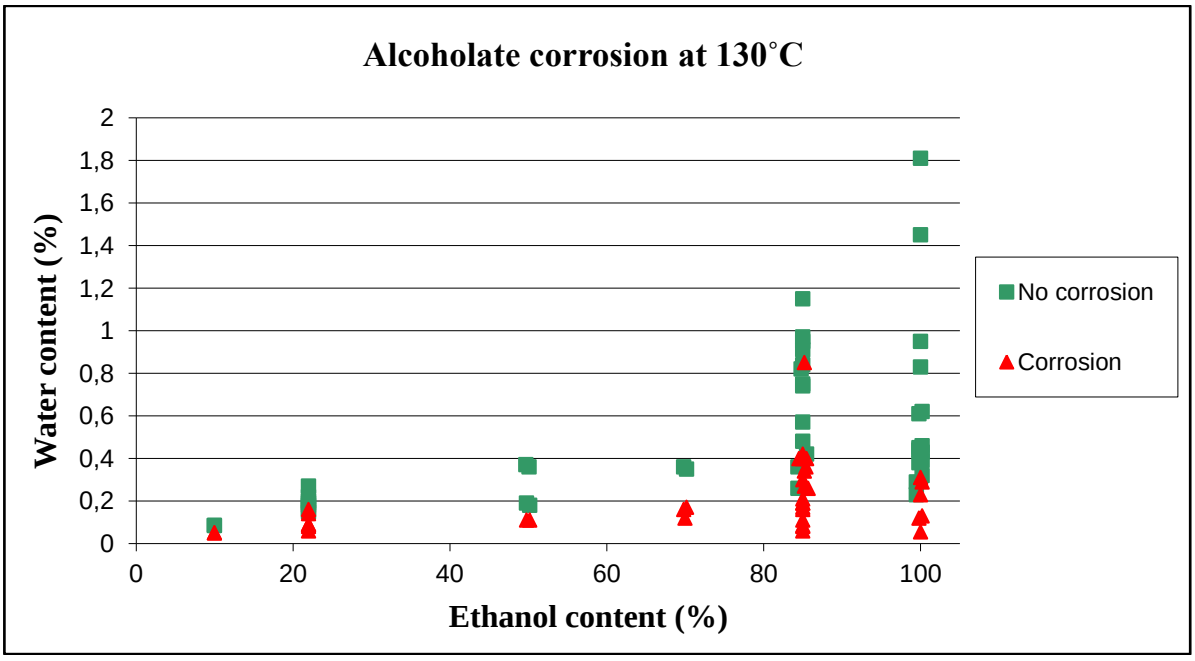

Figure 5.8. Water limit for alcoholate corrosion in ethanol blended fuels.

The water content from the fuels where no alcoholate corrosion had occurred was analysed for autoclaves with E85 and E100. The results from examining the water levels before and after testing are presented in Table 5.2. An increase of the water content was observed for all solutions. The mean values of the percentage increase of water content were 19% for E85 and 36% for E100. The samples were taken from ethanol exposure tests performed at the same time. Water content levels from other exposure tests also show a larger water increase of E100.

Solution	Water content before (%)	Water content after (%)	Increase (%)	Mean values (%)
E85	0.36	0.42	17	19
E85	0.42	0.50	19	
E85	0.48	0.63	31	
E85	0.57	0.67	18	
E85	0.74	0.82	11	
E100	0.45	0.59	31	36
E100	0.45	0.55	22	
E100	0.61	0.70	15	
E100	0.61	0.95	56	
E100	0.83	0.90	8	
E100	0.95	1.07	13	

Table 5.2. Water content before and after testing in E85 and E100.

5.2.1.2 Liquid and gas phase

Figure 5.9 show the results from the samples placed in contact with or above the ethanol solution. Samples of AA6063 in contact with the liquid showed a slight increase of the occurrence of alcoholate corrosion compared to the samples placed in the gas phase. A380 samples only became affected of alcoholate corrosion in contact with the liquid. The results show that the liquid phase is more corrosive than the gas phase. See Appendix II for data.

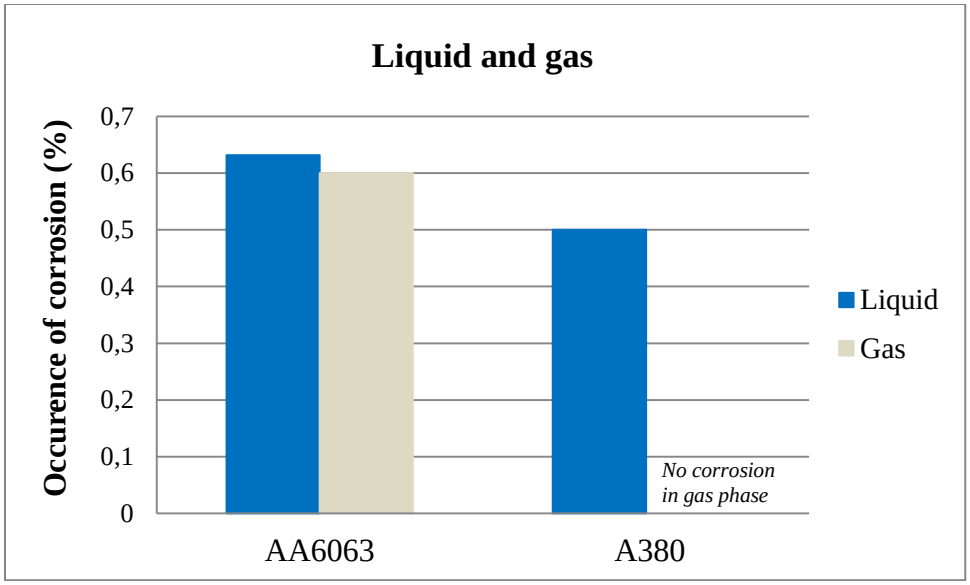

Figure 5.9. Occurence of corrosion of aluminium alloys exposed to E100.

5.2.2 Surface treatments

The results from the tests of AA6063 and surface treated AA6063 are summarised in Table 5.3, where an x-mark means that corrosion occurred. The test with a water content of 0.48% resulted in no corrosion in any of the autoclaves. At water content 0.26%, one autoclave with an anodised warm sealed sample and one autoclave with a AA6063 sample were affected by corrosion. At water content

0.18% one autoclave with Keronite and one with AA6063 were affected of alcoholate corrosion. One autoclave with Keronite was also affected at 0.19% and both autoclaves with AA6063.

Surface treatment	Autoclave	Water content (%)			
		0.48	0.26	0.18	0.19
Pure AA6063	1	-	-	-	x
	2	-	x	x	x
Anodised cold sealed with nickel	1	-	-	-	-
	2	-	-	-	-
Anodised warm sealed	1	-	x	-	-
	2	-	-	-	-
Keronite coating	1	-	-	-	-
	2	-	-	x	x
Nickel coating with medium phosphor content	1	-	-	-	-
	2	-	-	-	-
Nickel coating with high phosphor content	1	-	-	-	-
	2	-	-	-	-

Table 5.3. Results from testing of AA6063 and surface treated AA6063.

The affected AA6063 sample at a water content of 0.26% is shown in Figure 5.10. It presents an example of how the surface can look like after alcoholate corrosion. The voluminous corrosion products from the alcoholate corrosion reaction can be seen on the bottom (b). The corrosion products were first in a gel-like form and after time they became hard and brittle. On almost the entire surface small pits were visible.

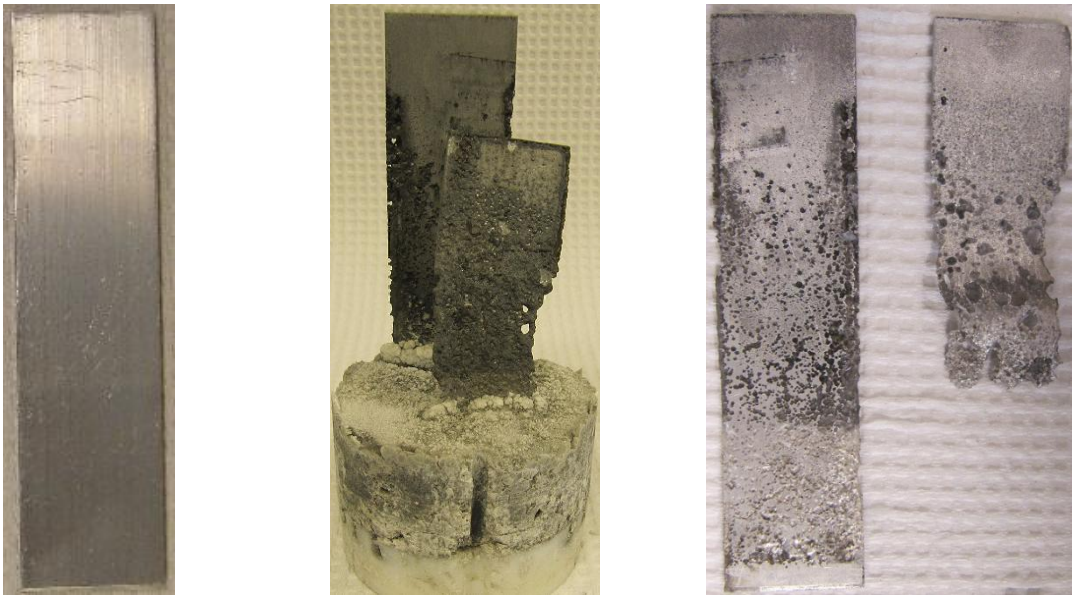

a **b** **c**

Figure 5.10. Aluminium alloy AA6063. a) Unexposed. b) Affected. c) Affected and washed.

Figure 5.11 shows LOM and SEM pictures of corroded AA6063 with small pits of different size distributed over the surface. The white corrosion products seen in b) are dried $Al(OH)_3 \times nH_20$ that has transformed into bayerite.

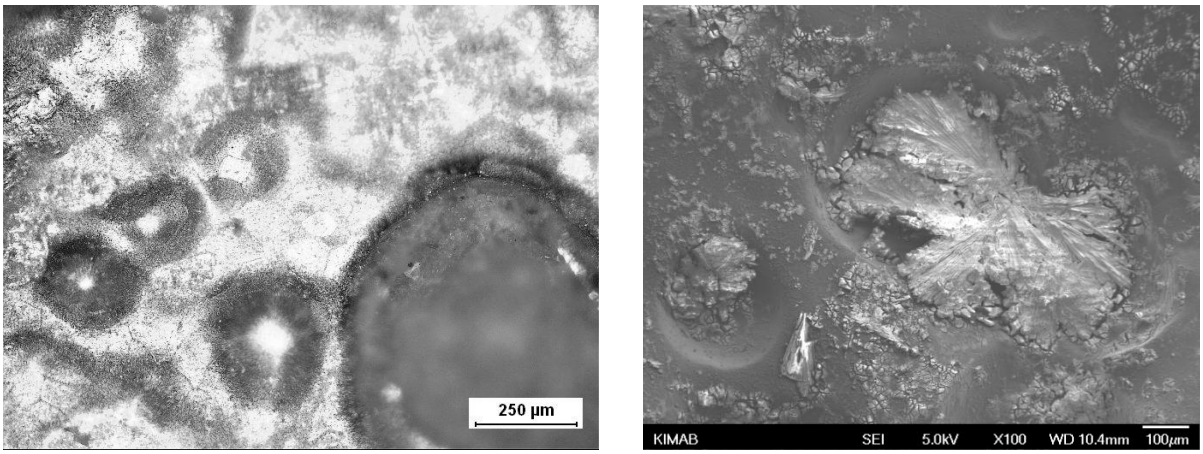

A **b**

Figure 5.11. AA6063 affected of alcoholate corrosion. a) LOM-picture. b) SEM-picture. 1 000x magnification.

In Figure 5.12 the appearance of the unexposed and exposed anodised warm sealed samples are shown. The corrosion of the anodised warm sealed sample was a mixture of filiform and alcoholate corrosion. A larger occurrence of corrosion was seen in connection to the edges, at the same areas where filiform corrosion was initiated. Filiform corrosion weakened the coating and the aluminium alloy became accessible for alcoholate corrosion and parts of the sample were destroyed.

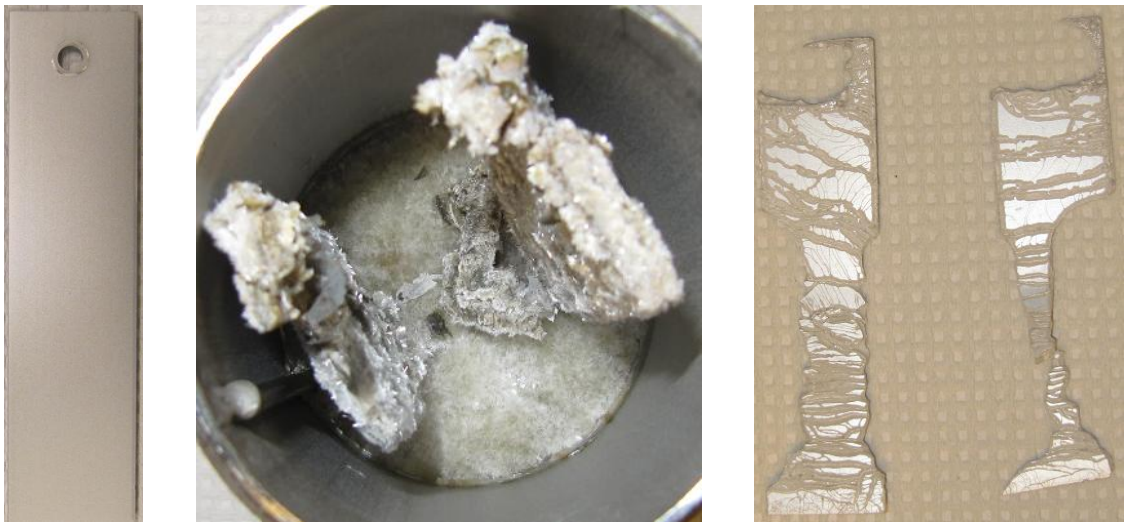

a **b** **c**

Figure 5.12. Anodised and warm sealed samples. a) Unexposed. b) Affected. c) Affected and washed.

Figure 5.13.a. shows a close up on the affected anodised warm sealed sample. It is possible to observe filiform corrosion filaments of different thicknesses across the surface. At different places in the filaments, marked with circles in a) and b), round holes indicate initiation of alcoholate corrosion.

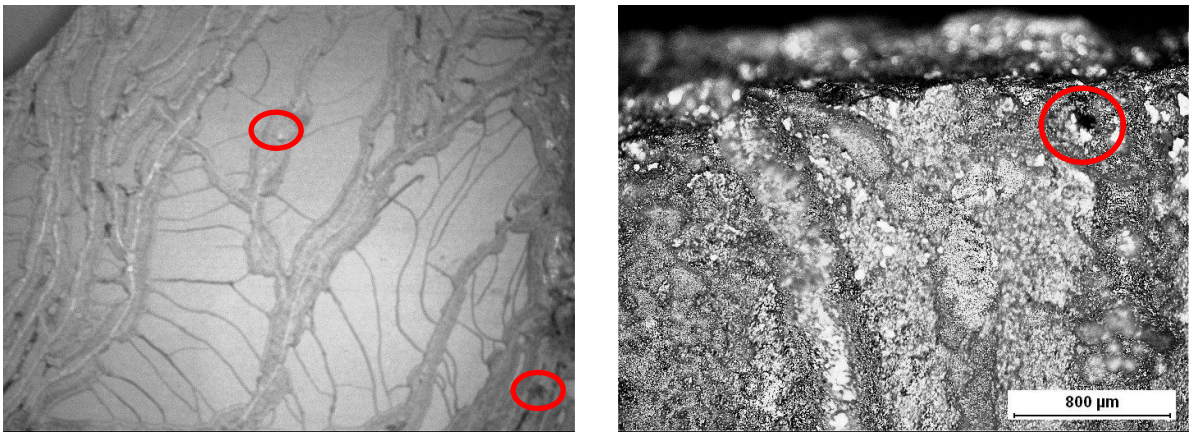

A **b**

Figure 5.13.a) Close up of affected sample. b) LOM picture of the edge. Red circles indicate where alcoholate corrosion has started.

Figure 5.14.a. show a SEM picture of a filament thread and b) a magnification of the corroded area. The corrosion area in b) shows a wide spread of holes on the surface.

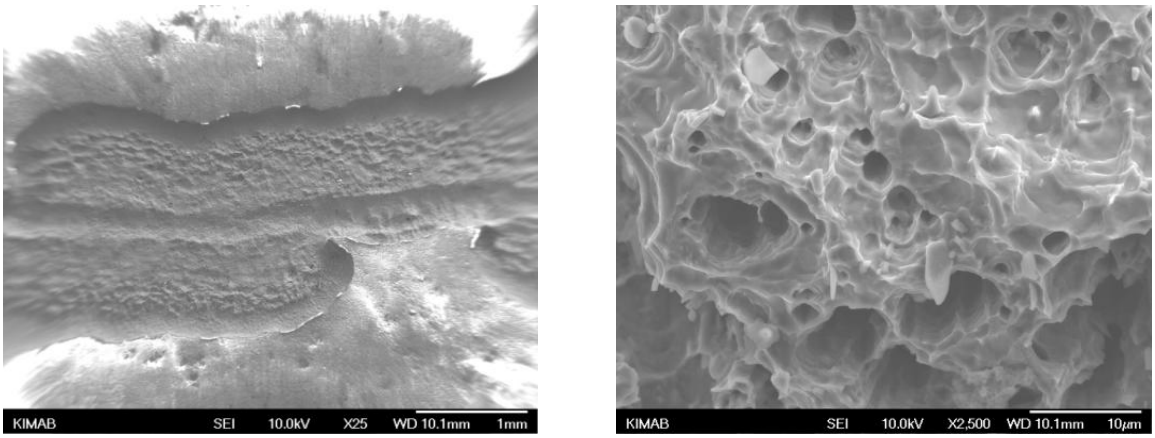

A **b**

Figure 5.14. SEM-pictures of filament thread. a) 25x magnification. b) 2 500x.

The tests executed at 0.18 and 0.19% gave alcoholate corrosion in one out of two autoclaves with Keronite samples. In Figure 5.15, Keronite affected to alcoholate corrosion at water content of 0.18% is shown. The alcoholate corrosion pits are randomly distributed all over the samples. Also for these samples corrosion was mainly taking place at the edges.

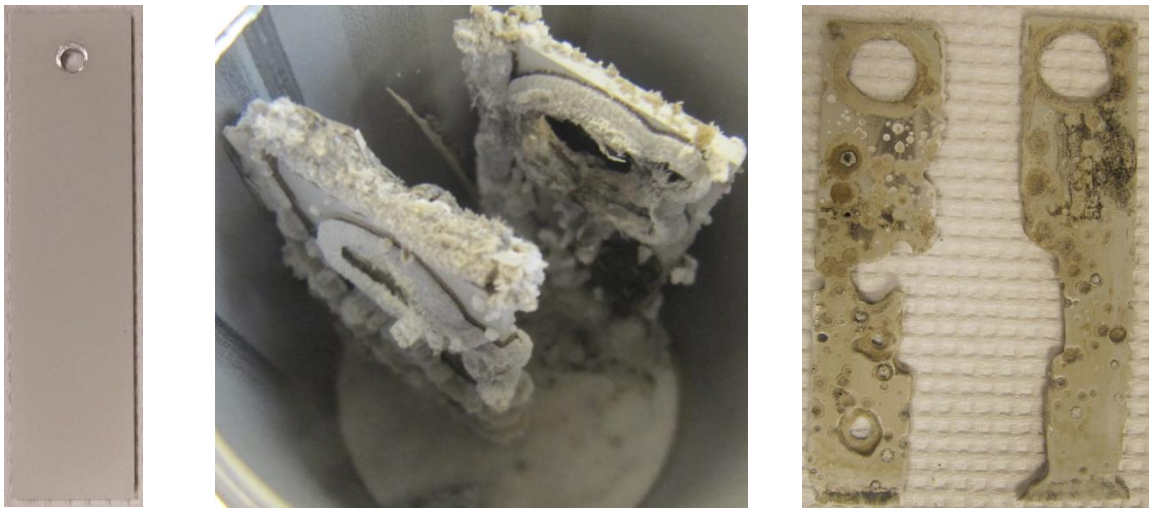

a **b** **c**

Figure 5.15. Keronite samples. a) Unexposed. b) Affected. c) Affected and washed.

Figure 5.16 shows close ups on the affected Keronite. The corrosion pits in a) are more frequent and show a less circular shape than the pits in b).

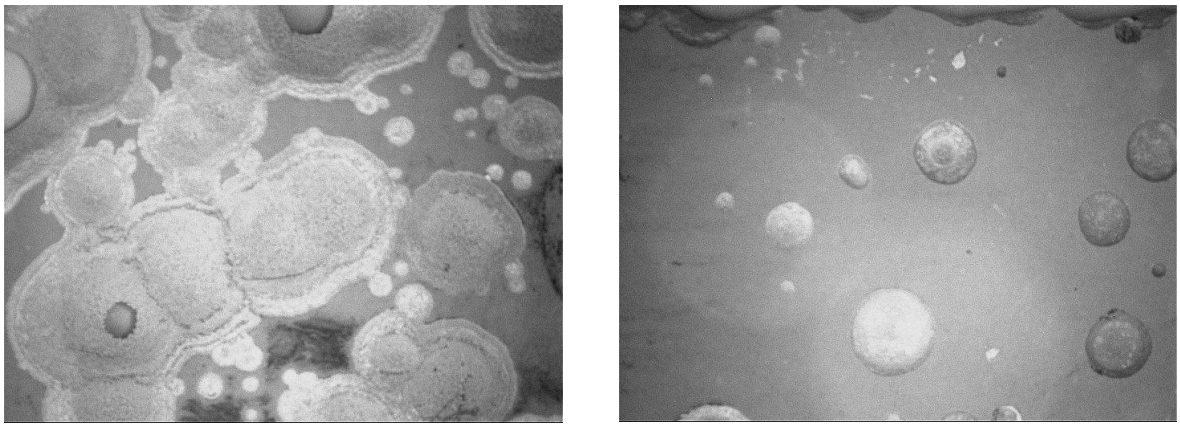

A **b**

Figure 5.16. Keronite samples affected of alcoholate corrosion at water content 0.18% (a) and 0.19% (b).

Figure 5.17 show the area of corrosion pits of the affected Keronite at water content 0.18%.

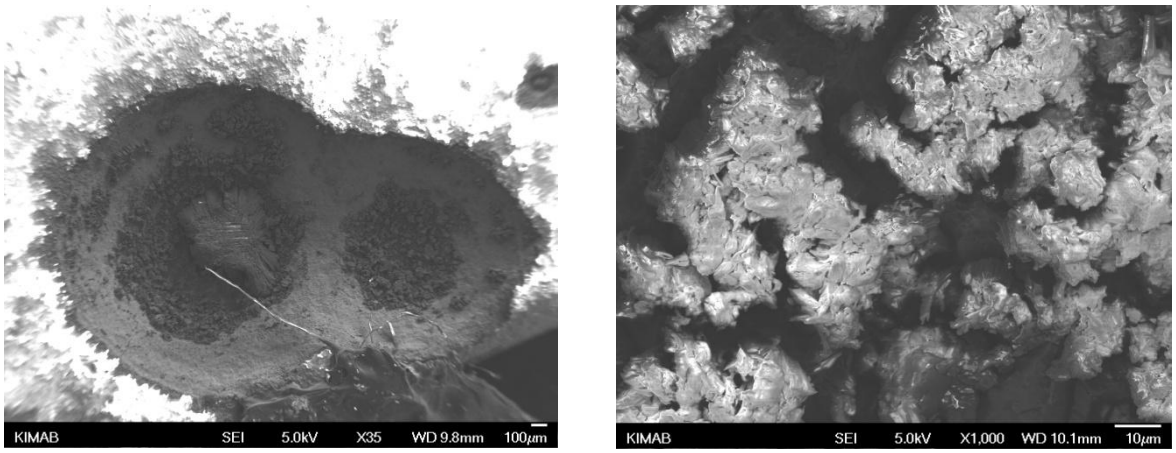

A **b**

Figure 5.17. SEM-picture of affected Keronite coating. a) 35x. b) 1 000x.

5.2.3 Temperature

Results from the temperature tests in autoclaves are presented in Figure 5.18 (see Appendix III for data). Each cluster of dots represents autoclaves that were exposed at the same time, temperature and water content. The figure shows an increase of occurrence of alcoholate corrosion at elevated temperatures. At lower temperatures the occurrence of corrosion is decreasing along with an increase of necessary time before corrosion.

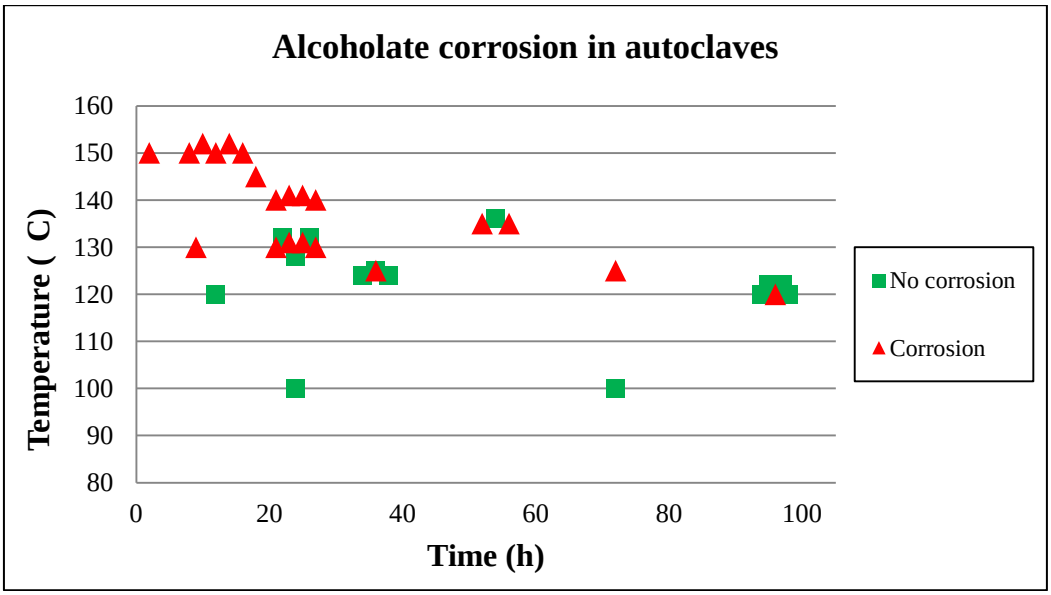

Figure 5.18. Temperature and time dependence for alcoholate corrosion of AA6063. The water content varies between 0.13-0.25%.

5.2.4 Time

Figure 5.19 and Figure 5.20 show the results from the logger tests. It shows that it takes longer time before alcoholate corrosion occurs at 130 °C compared to 150 °C. In the pressure test at 130 °C the pressure remained constant at 5 bar until an pressure increase started at approximately 500 minutes. For the test at 150 °C the pressure never remained constant and increased slowly until corrosion occurred after only ~110 minutes.

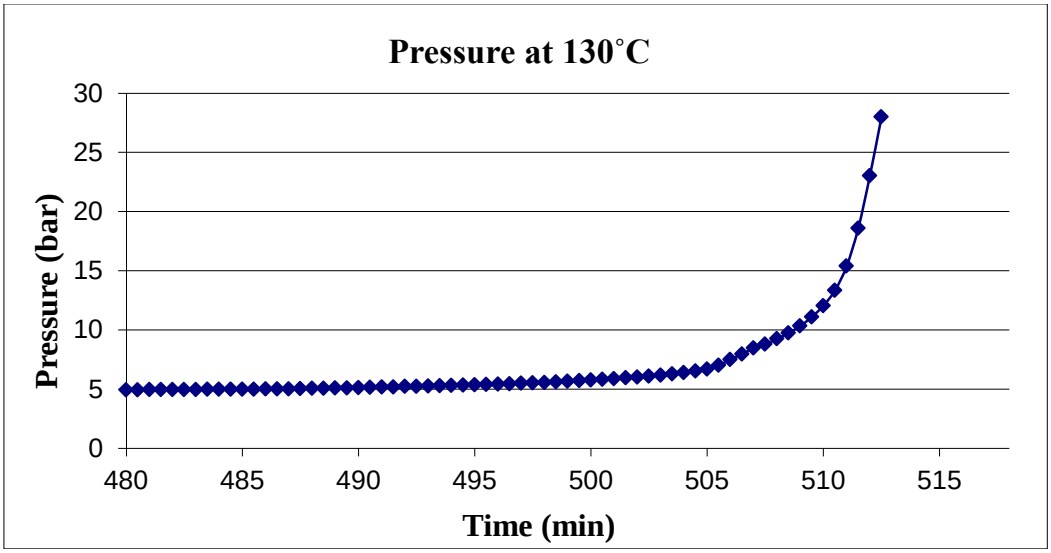

Figure 5.19. Time to corrosion at 130°C.

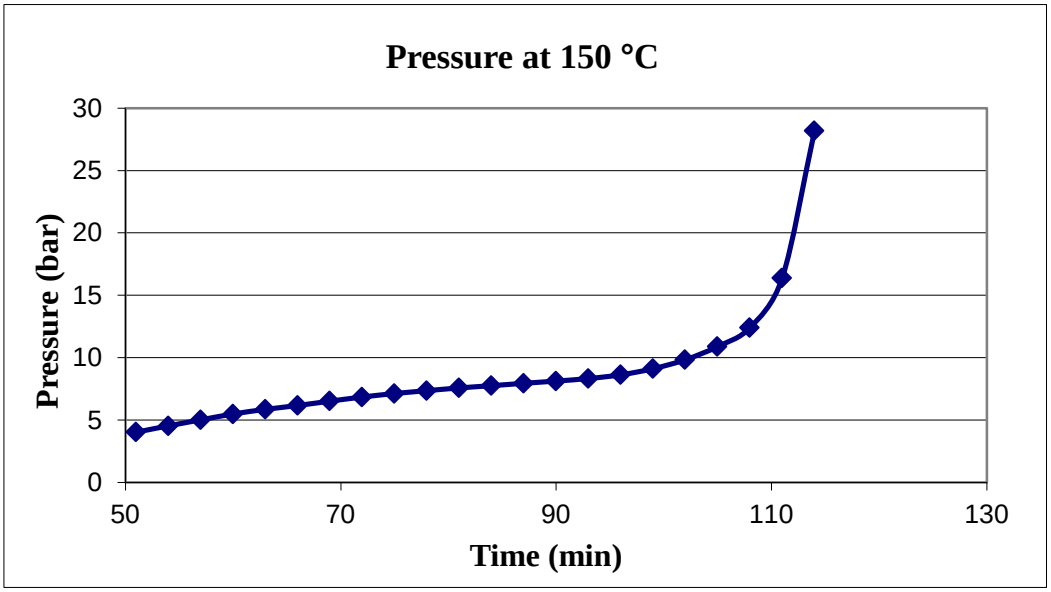

Figure 5.20. Time to corrosion at 150°C.

5.2.5 Pressure

To see additional data from the pressurisation tests see Appendix II.

5.2.5.1 Oxygen

Results from the oxygen pressurisation with AA6063 are shown in Figure 5.21. The figure shows that the occurrence of corrosion has been greatest in autoclaves at initial pressure of 1 bar and the occurrence decreased at higher initial pressures.

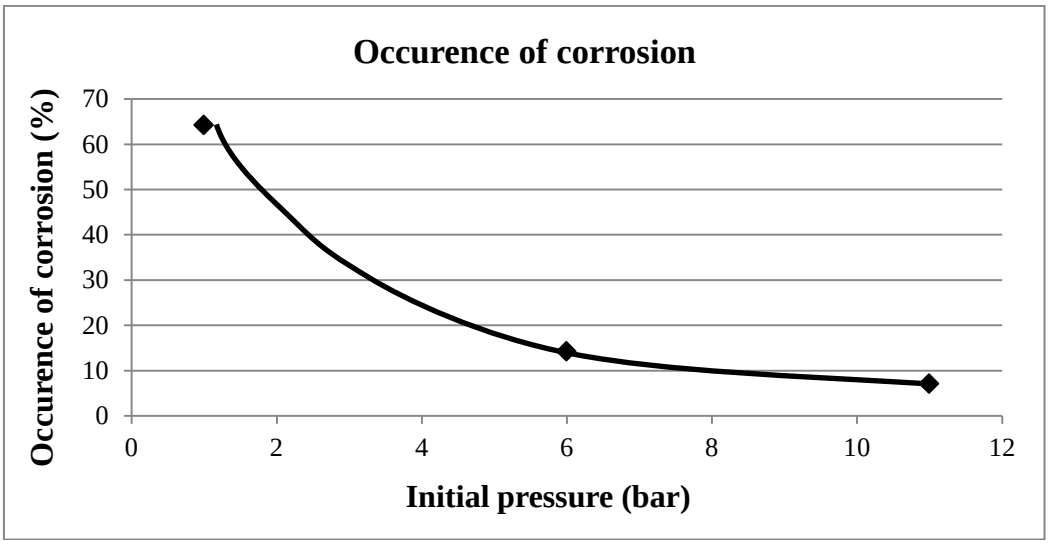

Figure 5.21. Occurrence of corrosion in oxygen pressurisation tests.

Liquid was taken from the unaffected autoclaves in the pressurisation test with oxygen. The liquids was analysed using Karl Fischer Coulometer and compared with corresponding initial water contents. Figure 5.22 shows a large increase in water content in relation to the initial pressure. The water content from the unpressurised autoclaves showed an increase of 95% and was quite small in relation to the pressurised autoclaves. At the highest pressure an increase of approximately 1800% was evident.

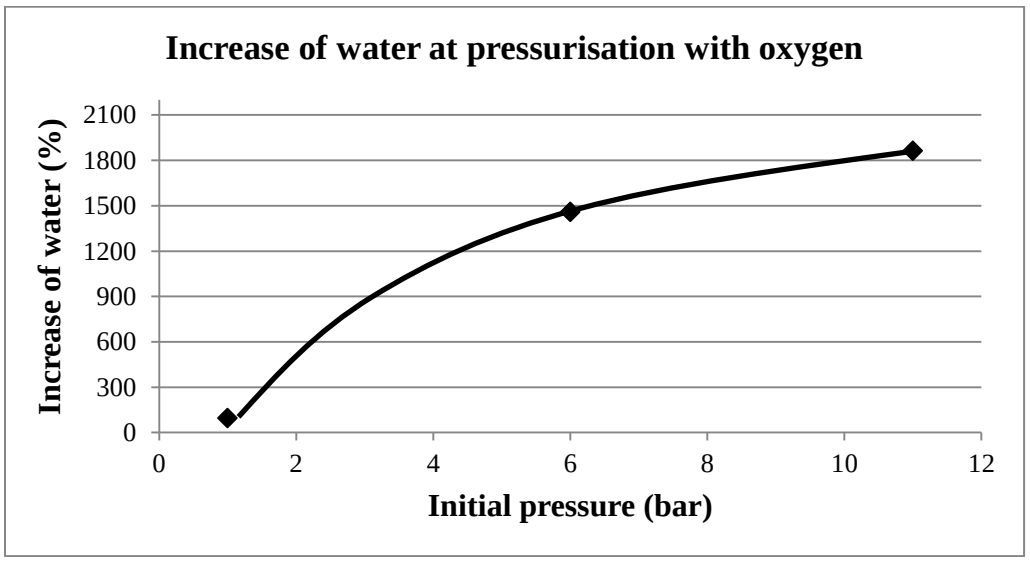

Figure 5.22. Increase of water in the ethanol depending on initial pressure.

5.2.5.2 Nitrogen

In Figure 5.23 the results from the pressurisation test with nitrogen is shown. This test was performed to a smaller extent and the increase at 6 bar correlated to only one more occurrence of alcoholate corrosion, compared to 1 and 11 bar. Consequently the pressurisation test with nitrogen showed an almost equal occurrence of corrosion between the three different pressures.

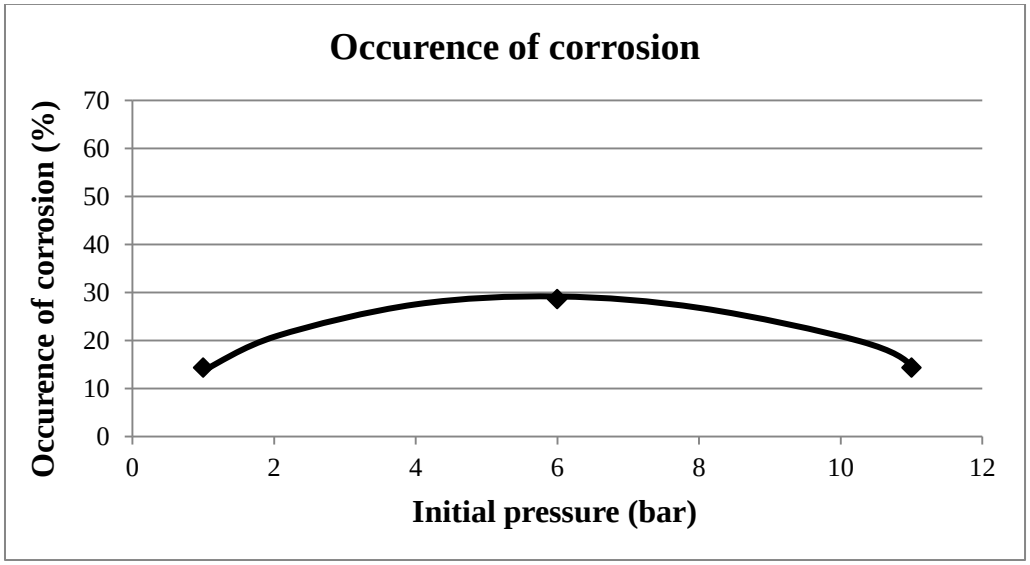

Figure 5.23. Occurrence of corrosion in nitrogen pressurisation tests.

The water content of an autoclave setup pressurised with nitrogen was analysed (see Figure 5.24). The unpressurised autoclave with no nitrogen pressurisation increased the water content by 28%. The autoclave with initial pressure of 6 bar increased the water content by 3% and the autoclave at initial pressure of 11 bar remained the same water content also after exposure.

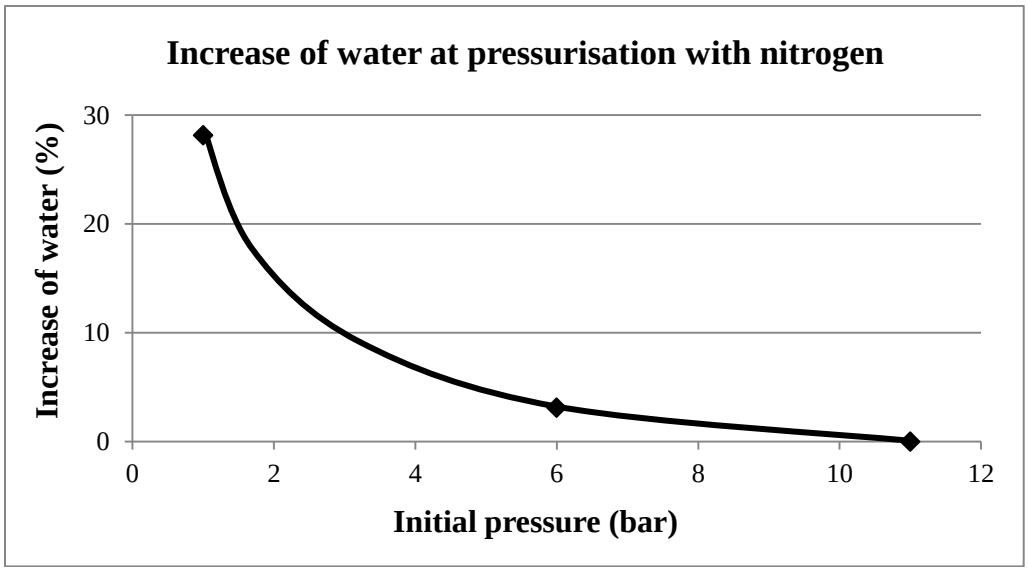

Figure 5.24. Increase of water depending on initial pressure. Notice the different scale compared to Figure 5.22.

5.2.6 Characterisation of corrosion products

FTIR was performed on corrosion products scraped from corroded samples. Figure 5.25 show how the alcoholate corrosion products can look. a) the standard appearance of alcoholate corrosion products before it has dried, b) corrosion products still moist and looking like gel-like grains and c) two corroded aluminium alloys surrounded of the gel-like corrosion products.

a b c

Figure 5.25. a) Gel of alcoholate corrosion product. b) Corrosion product in form of gel-like black grains. c) Affected samples in its alcoholate corrosion products.[64]

Figure 5.26 displays the infrared spectrum of ethanol. It shows the O-H-stretching vibrations at 3300 cm^{-1} and the O-H bond in range of 1600-1300 cm^{-1}. The C-H stretching bond can be seen at 3000 cm^{-1} and at 1050 cm^{-1} the C-O bond.[67]

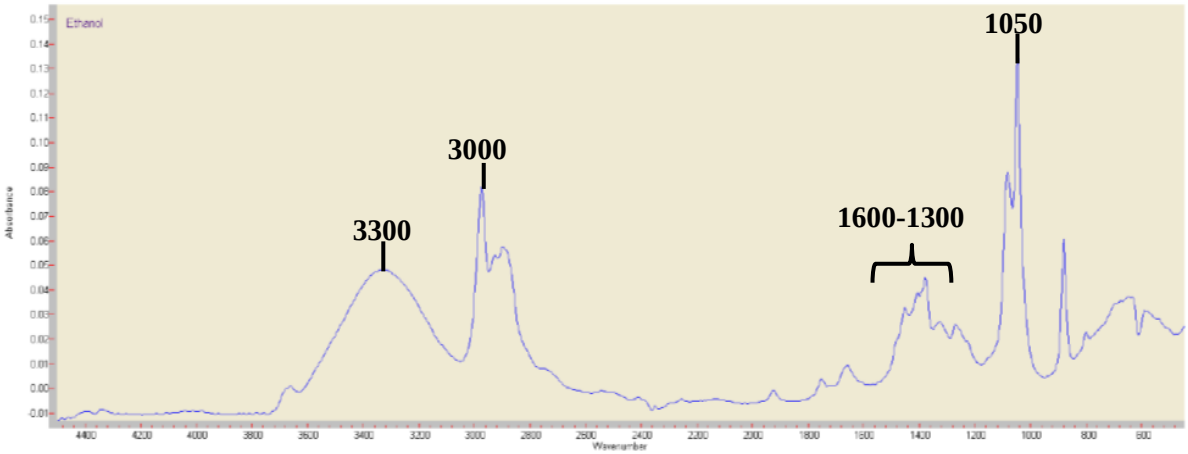

Figure 5.26. FTIR- spectrum of ethanol.[64]

In Figure 5.27 a spectrum is compared to a reference spectrum of aluminium alcoholate and in the figure the three highlighted peaks represent aluminium alcoholate, $Al(C_2H_5O)_3$. These results show that the corrosion product consists of aluminium alcoholate, as predicted from reaction (9).

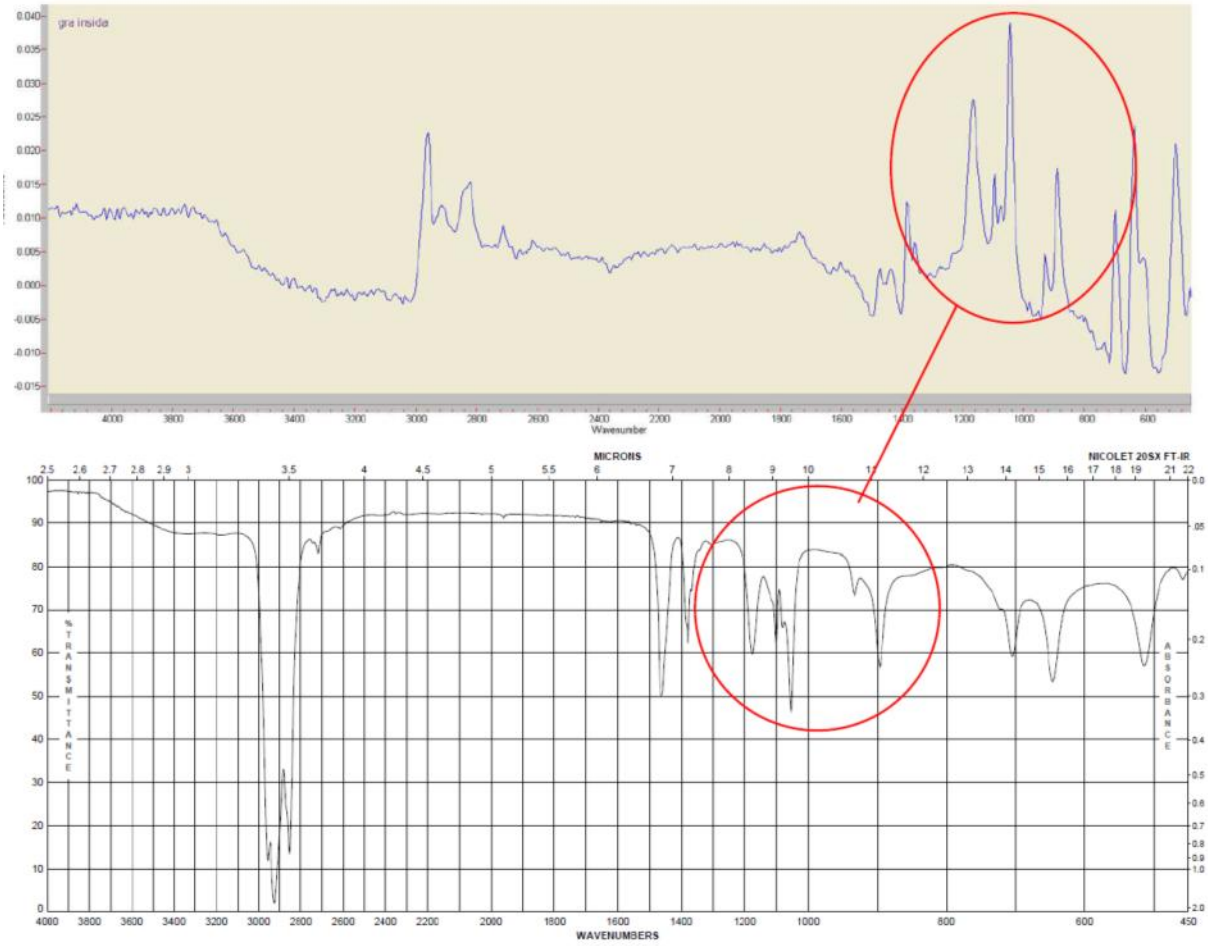

Figure 5.27. Comparison of corrosion products with reference spectrum of aluminium alcoholate. Typical peaks for alcoholate corrosion are marked.[64]

Figure 5.28 and Figure 5.29 show two typical spectra from the corroded samples. The three peaks of aluminium alcoholate can be seen marked in the figures. The largest difference between the spectra was the occurrence of peaks at 3300 cm^{-1} and in range of 1600-1300 cm^{-1} correlating to the O-H bond. These peaks in Figure 5.28 could be an indication of aluminium hydroxide, $Al(OH)_3$, and reaction (10). It can also be connected to the O-H bond peaks of ethanol.[67]

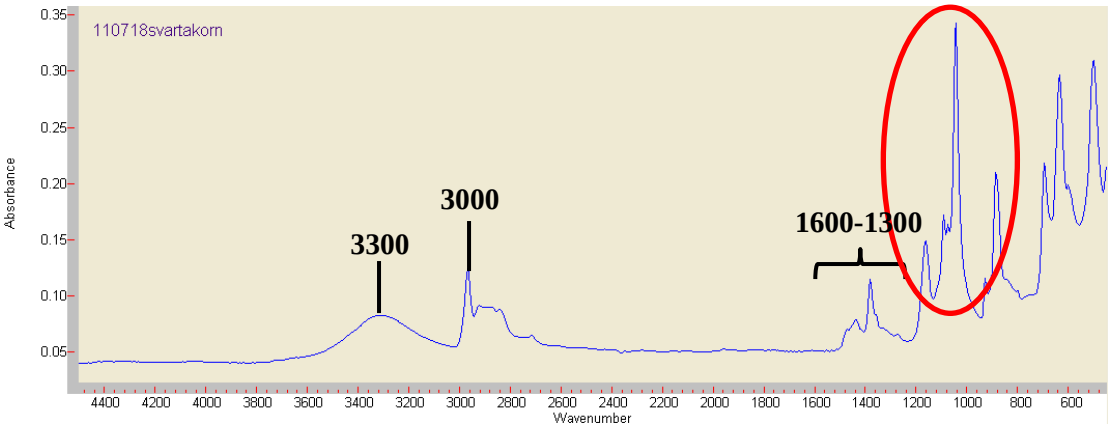

Figure 5.28. FTIR-spectrum of moist corrosion product sample. Aluminium alcoholate peaks are marked in the figure.

Figure 5.29 shows a sample of dried corrosion products. It shows the peaks of aluminium alcoholate and the C-H bond at 3000 cm $^{-1}$. Since the O-H bond is not present at 3300 cm $^{-1}$, the area in the range of 1600-1300 cm^{-1} reveals no O-H bonds.

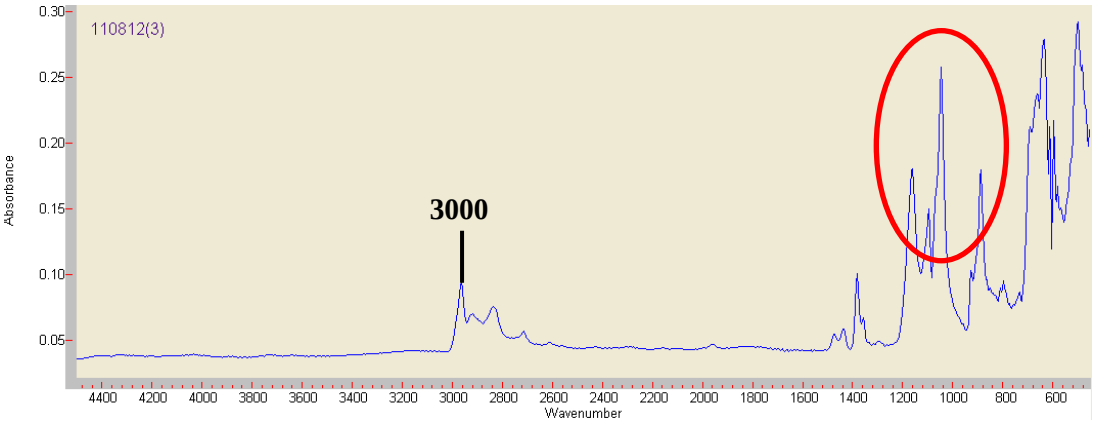

Figure 5.29. FTIR-spectrum of dried corrosion product sample. Aluminium alcoholate peaks are marked in the figure.

6 Discussion

Studies regarding aluminium exposed to alcohols have presented results of both pitting corrosion and alcoholate corrosion. In reported studies using anhydrous ethanol it has been noticed that what the authors denote pitting corrosion, sometimes seems to be alcoholate corrosion.[19, 53] Even though the authors realise that another mechanism than pitting corrosion must have occurred, the term pitting corrosion is still used. A wider knowledge of alcoholate corrosion seems to be required in the field of corrosion research.

6.1 Water dependence

When performing pressurisation tests with oxygen the autoclaves exposed to higher initial pressures showed lower occurrence of alcoholate corrosion. Measurements of the water content before and after exposure with oxygen showed a drastic increase of water in the ethanol solution (see results presented in Table 5.2). The explanation is probably that ethanol reacts with oxygen and form water, according to reaction (14). The higher amount of water in the ethanol solution prevents corrosion to occur during these conditions. The results from using nitrogen do not show this increase in water confirming the occurrence of reaction (14) in the oxygen tests.

6.1.1 Different fuel blends

The tests regarding the influence of water content upon alcoholate corrosion in different ethanol solutions show that a decrease in the water content results in an increased occurrence of alcoholate corrosion (see Figure 5.8). Figure 6.1 shows that alcoholate corrosion is almost certain in the zone (E85-E100) with <0.2% water content. At higher water contents, an exact line between a safe and unsafe area is not possible to establish since there seems to be an overlap in the occurrence of corrosion. However, the results indicate that above a water content of 0.5% no alcoholate corrosion should occur. For E85 with a water content of 0.82%, corrosion occurred in one autoclave. Corrosion at this high water level has not shown any repeatability and corrosion at this point ought to be seen as rare. Although the autoclave affected of corrosion at high water content was disregarded in the estimation of the critical water content limit it demonstrates that unpredicted circumstances can cause alcoholate corrosion.

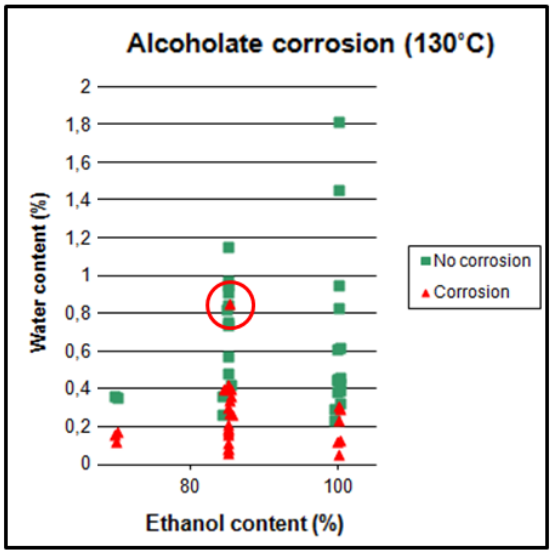

Figure 6.1. Focus on E85 and autoclave with water content 0.82 (from Figure 5.8).

Krüger et al.[19] conclude the critical water level of the ethanol blends E10, E25, E50 and E85 to be 0.2% water. This is consistent with the results generated in this study except for E85 and E100. The results show a somewhat higher critical water level of approximately 0.4% for these ethanol solutions. This could be correlated to the material characteristics in the different aluminium alloys tested.

Below E85 the water content level with risk of corrosion was indicated to be around 0.2%. This water content level seemed to slightly increase up to E85 and E100. Though, a slightly lower level was seen for E100 compared to E85. From the literature an increase in aggressiveness of alcoholate corrosion with higher ethanol content has been presented. In Figure 5.8 the water content of alcoholate corrosion is lower at E10 compared with E100 (this could however be due to less performed tests in E10 and are not statistically proved). The higher limit in E100 contributes to the statement that the ethanol content affects the occurrence of alcoholate corrosion. However, based on this theory, E100 should have been more corrosive than E85. The possible reduction from E85 to E100 in this study has however not been observed in earlier studies. The most probable reason for the dip from E85 to E100 is that E100 adsorb more water than E85. In Table 5.2 it has been shown that the solutions of E100 obtain higher amounts of water than E85. This correlates to ethanol being a hygroscopic liquid that absorb water from the surroundings. During the preparation for the ethanol exposure and during exposure, ethanol absorbed water from the surrounding air. The water content became higher than the selected water content and resulted in an inhibitory effect of the occurrence of alcoholate corrosion, and consequently in the lower water content limit in E100 seen in Figure 5.8.

The presence of MTBE in E85 could be another explanation for the slightly higher water content in E85. The MTBE and gasoline part of the solution might solve water and in consequence take water from the corrosive ethanol. The ethanol in the E85 solution could be left with lower water content and become more corrosive.

6.1.2 Liquid and gas phase

Results from the ethanol exposure showed an indication of a difference in corrosiveness in the liquid and the gas phase. A literature survey was performed to explore the possible reason for these results. In the literature it has been shown that the composition of ethanol and water solutions, because of their azeotropic nature, alters by temperature and pressure. It is therefore important to know how the ethanol and water solutions are affected by temperature and pressure. At low pressure and temperatures the composition of the liquid changes to another in vapour. As shown in Figure 6.2, area A is where the ethanol content is below the azeotropic point, <0.956. In this area the vapour consists of more ethanol than the liquid. Above the azeotropic point, B, the vapour consists of more water than the liquid. Boiling a liquid with a composition in area B would result in a liquid of lower water composition. This decrease in water content needs to be evaluated if it could be enough to result in a more corrosive ethanol that could cause alcoholate corrosion.

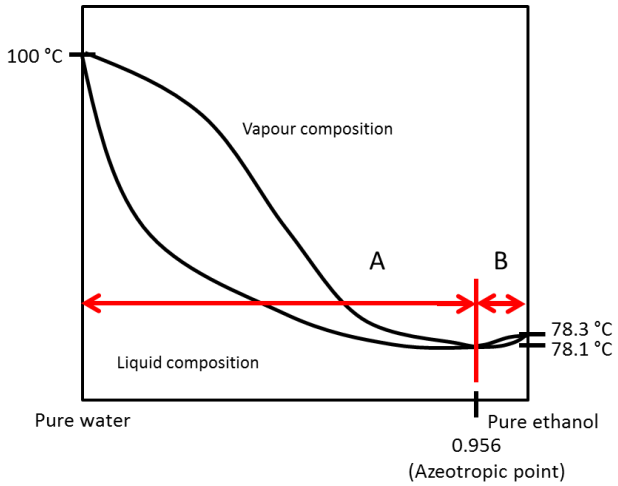

Figure 6.2. Vapour and liquid equilibrium of ethanol and water at 1 bar.

A possibility to influence the liquid and vapour differences is by changing the pressure and the temperature. Previously performed studies [41, 43-47] of pressure measurements of ethanol and water solutions show how a higher temperature and pressure result in smaller compositional differences between the liquid and the vapour. An increase in temperature and pressure has shown the azeotropic point to move to lower ethanol content. An increase high enough has even shown to eradicate the zone above the azeotropic point (side B in Figure 6.2).

To explore the azeotropic effect of alcoholate corrosion the ethanol exposure tests with different fuel blends the autoclaves with only ethanol and water (E100) were examined. The water contents in the tests were in range of 0.12-1.81% and the area of occurrence of alcoholate corrosion was at water in range 0-0.4%. The area of uncertainty of alcoholate corrosion can in Figure 5.8 be seen to approximately be in range of 0.2-0.4% water. This means that in an interval of around 0.2% it is uncertain if corrosion will occur or not. This would indicate that for the azeotropic properties to be of significance for the occurrence of alcoholate corrosion, the difference in composition of the liquid and the vapour should affect this 0.2% interval.

In Figure 6.3 the ethanol and water azeotrope at high ethanol content is shown at atmospheric pressure. Above the azeotropic point a higher initial ethanol content will result in less water in the vapour. The distance between A-D and E-H gives the difference in the composition of the liquid and the vapour. The distance between A-D is shorter than E-H showing that higher ethanol content gives a smaller difference in the composition of liquid and vapour. In a solution of high ethanol content the water content will not decrease as much as in a solution with lower ethanol content. That means that higher ethanol content result in a smaller compositional difference between the liquid and the vapour.

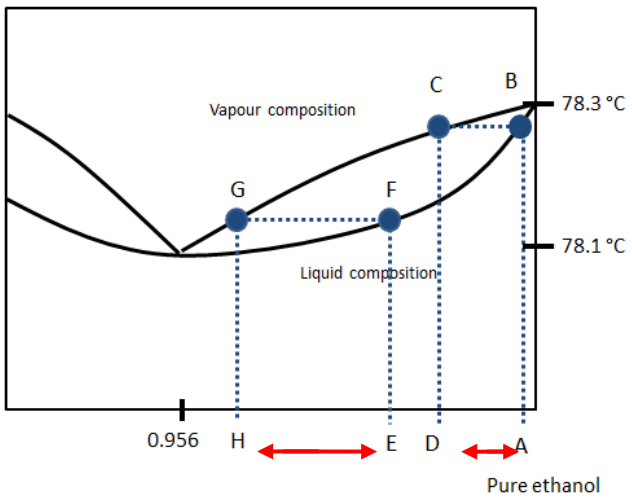

Figure 6.3. Composition difference (figure not to scale, initially Figure 1.10).

At atmospheric pressure the azeotropic point is at a 95.6% ethanol content and 4.4% is how much part B (see Figure 6.2) consists of. For alcoholate corrosion to occur the critical water level has been showed to be approximately at 0.4% for E100. For alcoholate corrosion to occur the ethanol solution needs to consist of 99.6% ethanol or more. At this ethanol content the difference between the liquid and the vapour is minimal but significant. Values at 150°C and almost 10 bar showed a slight difference at the ethanol and liquid solution at 96.6% ethanol.[41] The vapour contains 96.1% ethanol providing a difference of 0.5%. This means that a solution of 96.6% ethanol can result in a decrease of 0.5% water in the liquid. The liquids in this study consisted of high ethanol content above 99.5%. For something close to 0.2% of water to evaporate from the liquid to vapour is quite unlikely. In connection to the tests performed by comparing the liquid and the gas phase, a connection to the liquid being more corrosive than the gas has been seen. This could be because the azeotropic properties make the liquid more corrosive. Alcoholate corrosion occurred at low water contents and a small difference in the composition, providing that a higher ethanol content could be enough for the corrosion to take place.

The azeotrope might not be the only reason for alcoholate corrosion to start. The most probable reason for the corrosive difference between liquid and gas is that liquid consist of more ethanol. The higher level of ethanol in the liquid phase provides a greater opportunity for reaction (1) to occur.

6.2 Surface treatments

The comparison between the untreated AA6063 and the surface treated AA6063 samples show that the coatings help to prevent, or at least elongate the time before alcoholate corrosion starts. Each surface treatment showed improved results compared with the untreated AA6063. The only samples that were not affected by corrosion were samples containing nickel; the anodised and cold sealed with nickel and the nickel coatings with medium and high phosphor contents.

At a water content of 0.26%, one of the two autoclaves with anodised warm sealed samples was corroded. The corrosion is thus a combination of alcoholate corrosion and filiform corrosion. The surface tension makes the coating more sensitive at the edges where filiform corrosion starts, as illustrated in Figure 6.4. It is possible to see how the filaments have started at the edges and propagated across the samples. The filiform corrosion makes the aluminium accessible for the ethanol solution and the chemical reaction of alcoholate corrosion can occur. The surface affected by filiform corrosion is displayed in Figure 5.14.b) and showed holes that could be pores from the anodisation

process. Open pores would help the attack of alcoholate corrosion to occur and some of the holes seen in the picture may be pits of alcoholate corrosion.

Chlorides are reported necessary for filiform corrosion to occur. In this study no chlorides were used or no knowledge of any contact with chlorides known. This opens-up for speculations why filiform corrosion has occurred on the anodised warm sealed sample. A possible reason is that the ethanol solution has reacted and formed an acid, like acetic acid which provides a favourable environment for filiform corrosion to occur. More testing and research is necessary to conclude whether filiform corrosion was induced by the presence of some sort of defects in the sample or if this surface treatment is sensitive to filiform corrosion and then also consequently sensitive to alcoholate corrosion.

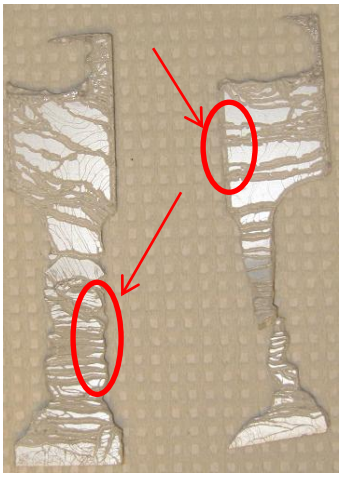

Figure 6.4. Corrosion starting at the edges.

It is noteworthy to compare the two anodised samples. They were sealed differently and the reason of corrosion of the warm sealed could be because of defects on the surface. If the sealing is insufficient, the pores from the anodisation act as initiation points for corrosion. This means that the cold sealed samples with the nickel coating could also be affected by corrosion if the sealing is insufficient. Another notion is that it is because of the nickel sealing that no corrosion occurred. The sealing with nickel and fluorine works as a barrier and this might be stronger than the barrier from the warm sealing.

In Figure 6.5 the alcoholate corrosion of Keronite coatings is shown. Comparing the two samples they look very similar, a) less and smaller pits compared to b) (see the red circles). If the corrosion in a) would have continued a while longer it probably would have looked like b). These two figures seem to give an indication on how the corrosion process proceeds. The Keronite coating is not sealed like the anodised coatings and can have some micro-cracks or open pores down to the aluminium substrate that can form during the surface treatment. These micro-cracks or open pores have become attacked and small alcoholate corrosion pits have occurred. The attack is propagating in the corrosion pits and the corrosion expands from the holes. The roundness of the alcoholate corrosion pits suggests that the samples probably were not affected by micro-cracks.

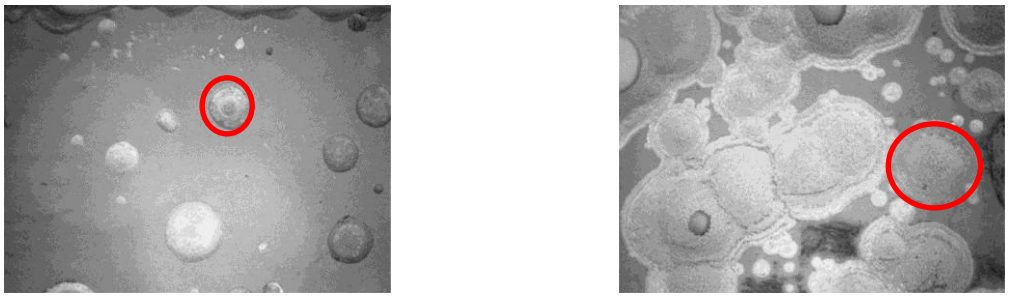

a b

Figure 6.5. Affected Keronite samples. a) 0.19% water content. b) 0.18% water content. The red circles point out the different sizes of the corrosion pits.

At the water contents of 0.18 and 0.19% the tests executed on Keronite samples resulted in alcoholate corrosion in one out of two autoclaves, respectively. This gives a reason to be concerned when using Keronite together with ethanol of low water content. Though it is important to be aware that the Keronite coating seems to be vulnerable for alcoholate corrosion, it appears as the coating help to prevent alcoholate corrosion in some extent. When uncoated AA6063 is affected of alcoholate corrosion, the attack is seen over the whole sample, almost without any unaffected area left. The corroded Keronite samples show large areas without any attack (see Figure 6.6). It seems like the coating hold back the progression of the alcoholate corrosion.

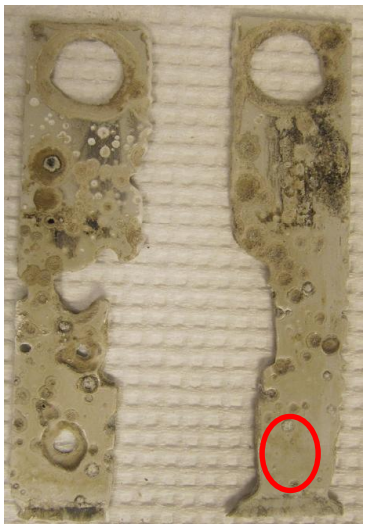

Figure 6.6. Alcoholate corrosion on Keronite coating. Area unaffected of alcoholate corrosion is marked.

The anodised and cold sealed sample with nickel and the two nickel coatings showed the best results. These three coatings did not indicate any sign of corrosion induced by exposure to the ethanol solutions. These findings are in concordance with findings of Krüger et al.[19] who showed chemically deposited nickel coatings to possess good qualities to prevent alcoholate corrosion. The anodised and sealed nickel samples were sealed with a nickel and fluorine composition. This composition can be assumed to be very good at preventing alcoholate corrosion since the sealing seems to have protected the substrate. The nickel coatings, which are electroless nickel platings and contain nickel and phosphor, showed a resistance towards alcoholate corrosion. These observations correlated to literature findings.

The cross section images of the nickel coatings showed a difference in coating thickness. The coatings were, according to the manufacturer, supposed to have the same thickness but the coatings with high

phosphor content were twice as thick as the coatings with the medium phosphor content. Differences in thickness affect influence their barrier protection and the difference in nickel and phosphor composition becomes of less importance. The coatings were set apart with the thicker coating providing a thicker barrier for any attacks to penetrate.

The samples of the nickel coatings and the anodised samples with nickel showed the best protective qualities. It is nevertheless important to remember that these coatings are sensitive to defects. Nickel coatings can result in unfavourable cathode-anode reactions and an anodised sample that has not been sealed properly can be highly corroded. Nickel seems to help to hinder the occurrence of alcoholate corrosion. The Keronite coating could be improved by using nickel as an impregnation agent. This might help the Keronite coating to get a thicker barrier against alcoholate corrosion.

6.3 Temperature and time

The tests performed have showed that there seems to be a relation between the temperature and the time before the start of alcoholate corrosion. Figure 6.7 shows that higher temperatures result in shorter time for corrosion to occur and vice versa. The water content of ethanol was quite similar in all of the tests except for two cases. In these two cases the water content was higher but the samples were still affected by alcoholate corrosion. In one of these cases, marked in Figure 6.7, the test temperature was of 150 °C and the start until alcoholate corrosion was still rapid. Due to this it is not likely that the higher water content has influenced the results. In the other case the ethanol with higher water content was tested at 125 °C and the time to corrosion was longer. This correlates to the relationship between temperature and time, a lower temperature results in a longer time to before the start of corrosion. However, it is still a possibility that the higher water content could have influenced the results. The higher water content could have moved the triangular dot to longer times and if the water content had been lower the time to corrosion could have been shorter.

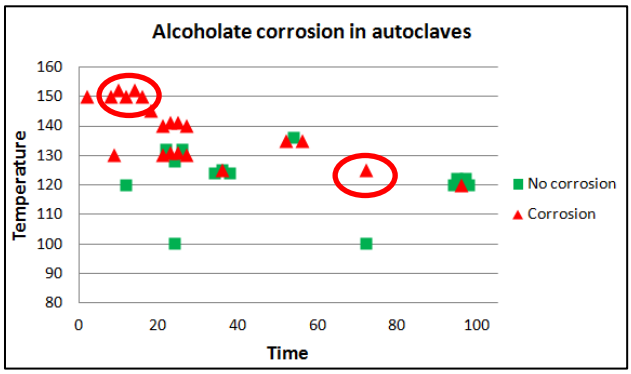

Figure 6.7. Occurrence of alcoholate corrosion (originally Figure 5.18).

In the logger tests this relation between the temperature and time parameters was clearly shown. The time to alcoholate corrosion was longer at lowered temperatures.
Exactly at how low temperatures alcoholate corrosion can occur and how long time that is necessary before corrosion occur cannot be evaluated from the short term testing. However, it is possible to observe a relation between lower temperatures and longer times. Krüger et al.[19] have showed that alcoholate corrosion can occur at 60 °C after 336 hours of exposure. This correlates to the assumption that a longer time of exposure is required at lower temperatures before alcoholate corrosion occur.

The temperature was defined as the predominant parameter governing alcoholate corrosion compared with time. A high temperature could rapidly result in an instant destructive alcoholate corrosion process. Nevertheless it is important to consider that a situation with low temperature after a sufficiently long time also could result in alcoholate corrosion.

The fact that the temperature influences the occurrence of alcoholate corrosion is quite straightforward. It has been known for a long time that the rate of chemical reactions varies with temperatures. In 1889 Arrhenius gave an interpretation of this fundamental knowledge in the Arrhenius equation[55]. The equation has shown to be very accurate on chemical reactions and from the equation it is possible to calculate that an increase in temperature results in an increase in the reaction rate constant. This correlates to how alcoholate corrosion occurred in the tests of this study since this type of corrosion attack is a chemical reaction.

The Arrhenius equation is not dependant on time so why alcoholate corrosion is affected of time is of great interest. It could be associated to the incubation time mentioned in the literature. The incubation time is how long it takes for specific anions in the solution to attack the passive oxide layer before it locally may break. The rate of this partial destruction is probably influenced by the temperature. This

theory is consistent with what is known about the oxide layer of aluminium. Higher temperatures have shown to influence the layer negatively.[5] A most likely theory of the reason time affects the occurrence of alcoholate corrosion is that time is necessary to destroy the passive oxide layer.

Temperature has showed to affect alcoholate corrosion but in all of the temperature tests pressure is also an important parameter. When the temperature increase the pressure also increase. The autoclave testing used in this study provides a closed system where that the pressure follows the temperature. In consequence no unique temperature tests were possible.

Another aspect in correlation to the dependence of alcoholate corrosion at elevated temperatures is that no corrosion has been observed at room temperature. Pitting corrosion on the other hand can occur at room temperature. This together with the results from the FTIR analysis of corrosion products strengthens the conclusion that alcoholate corrosion occurred and not pitting corrosion.

6.4 Pressure

The pressure tests with oxygen showed a difference in the probability of corrosion depending on the initial pressure. Figure 5.21 shows a reduced occurrence of alcoholate corrosion along with an increased initial pressure. Reaction (14) in 1.3.4 shows that ethanol and oxygen can form water, a reaction that can be related to the increase of water at higher pressures, see Figure 5.22. This water increase could be the reason of the decrease of alcoholate corrosion at higher pressures. For this reason the lower occurrence of corrosion at higher pressures from oxygen pressurisation needs to be considered with caution.

The tests performed with nitrogen showed results slightly in the opposite direction. The pressurised test with nitrogen resulted in a lower increase of the water content at higher pressures. This means that the nitrogen did not affect the ethanol and water composition as much as the oxygen. The pressurised tests with nitrogen showed a slight increase of corrosion at 6 bar.

This could mean that a higher pressure affects the occurrence of alcoholate corrosion. The reason could be that a fast increase in pressure develops when alcoholate corrosion occur. An initial increased pressure could influence the corrosion to occur or result in a shorter time before corrosion occurs. The pressure could also make the passive layer easier to attack- A situation that would not lead to alcoholate corrosion could develop because of an increased pressure. The test with nitrogen were not as extensive as the test with oxygen and to definitely decide if the pressure influence the occurrence of corrosion, more tests would have been preferred.

6.5 Characterisation of corrosion products

To find the different bonds involved in the chemical reaction of alcoholate corrosion, the spectra of the corrosion products were analysed. Reaction (9) is the first and most important reaction producing the alcoholates of the alcoholate corrosion. The ethanol and aluminium reaction which produce aluminium alcoholate, $Al(C_2H_5O)_3$, and hydrogen, H_2 was confirmed in the spectra showing the three main peaks of aluminium alcoholate. The visual colour of generated alcoholate corrosion products did not show any effect on the spectra in relation to the aluminium alcoholate or the two other reactions. These two reactions, hydrolysation and decomposition of the aluminium alcoholates, were also studied.

Reaction (10) hydrolyse aluminium alcoholate together with water to aluminium hydroxide, $Al(OH)_3$, and ethanol. The O-H bond seen in the spectra correlated to the reaction. This O-H bond was also present in ethanol and water making it hard to conclude their origin. Although the corrosion samples analysed with FTIR had different moisture level and different appearances (see Figure 5.25), the

spectra were very similar. The spectra showed that mainly the O-H bond varied while the aluminium alcoholate peaks stayed constant. As described in the literature study part 1.3.1, the hydroxides together with aqueous solutions form gels. These gels upon aging eventually form bayerite. It seems like the spectra of the gel and the bayerite were relatively similar, except for the amount of O-H.

In reaction (11) the aluminium alcoholate is decomposed to aluminium oxide, Al_2O_3, ethylene, C_2H_4, and water. These could not be definitively determined in the spectra of corrosion products. The Al-O bond for the aluminium oxide is positioned above 900 cm^{-1} and could not be determined because of other overlapping contributions-. The C-H bond of ethylene was not observed at 1600 cm^{-1},probably because it is was not stable and could easily dissolve.[67]

7 Conclusions

- After water, temperature and time seem to be the main parameters governing alcoholate corrosion.

- No alcoholate corrosion should occur for aluminium alloy AA6063 exposed in one week at 130 °C in different ethanol fuel blends if the water content exceeds 0.5%.

- Pressurisation with oxygen results in a higher water content in the fuel and consequently a lower risk for alcoholate corrosion.

- No effect of pressure could be seen using an inert nitrogen gas.

- The surface treated aluminium alloy AA6063 resisted alcoholate corrosion better compared with AA6063 without any surface treatment.

- Electroless nickel plating assisted in the prevention of alcoholate corrosion.

- Keronite in an environment of ethanol with low water content can be affected of alcoholate corrosion.

- Alcoholate corrosion is a chemical reaction. Liquids with high water content inhibit alcoholate corrosion. High water contents can result in electrochemical corrosion processes, and low contents in chemical reactions. It is important that the water content in ethanol in the future is stated when known to be in contact with aluminium.

8 Future work

At the time of the testing of the coated samples the lowest possible water content obtained was 0.18%. As the testing was performed during the summer period, the air had a high humidity that made it difficult to reduce the water content further. It would be interesting to explore lower water contents. Since Keronite was susceptible to alcoholate corrosion in one out of two samples at water contents of 0.18 and 0.19%, it would be interesting to distinguish if a lower water content would give result in a higher influence on corrosion. More tests should be carried out to examine if the 50% risk of alcoholate corrosion is accurate or not.

It would be of interest to explore if the anodised and cold sealed samples are vulnerable to filiform and alcoholate corrosion.

A suitable further study would be to investigate the occurrence of alcoholate corrosion at pressurized tests and when testing surface treated aluminium alloys over a longer time period.

Higher temperatures seem to affect the oxide passive layer negatively. How the oxide layer is affected by the ethanol solution could be of interest to explore.

9 Acknowledgements

First of all I would like to thank my supervisors Ingegerd Annergren and Annika Talus at Swerea KIMAB for all of their support and guidance during this project. I also want to thank my supervisor Inger Odnevall Wallinder at KTH for her support. Thank you to all my co-workers at Swerea KIMAB for all the help and time you have given me and special thanks goes to Dan Persson and Christer Eggertsson. Finally I would like to thank the industrial members of the project "Materials in Biofuels" supplying this project.

10 References

1. A Literature Review Based Assessment on the Impacts of a 10% and 20% Ethanol Gasoline Fuel Blend on Non-Automotive Engines, in Analysis of Impacts. 2002, Orbital Engine Company.
2. Park, I.J., et al., Corrosion characteristics of aluminum alloy in bio-ethanol blended gasoline fuel: Part 2. The effects of dissolved oxygen in the fuel. Fuel, 2011. **90**: p. 633.
3. Toyota Motor North America, I. 2009: Washington D.C. p. 1-5.
4. Park I.J., Y.Y.H., Kim J.G. , Kwak D.H. , Ji W.S., Corrosion characteristics of aluminium alloy in bio-ethanol blended gasoline fuel: Part 2. The effects of dissolved oxygen in the fuel. Fuel, 2011. **90**: p. 633-639.
5. Vargel, C., Corrosion of Aluminium. 2004, Paris: Elsevier. 648.
6. Talbot, D. and J. Talbot, Corrosion Science and Technology. 1998, Boca Raton: CRC Press LLC.
7. Spoelstra, M.B., E.P.M. Van Westing, and J.H.W. De Wit, Characterisation of unsealed anodic oxide layers on aluminium. Werkstoffe und Korrosion, 2001. **52**(9): p. 661-666.
8. Miller, W.S., et al., Recent development in aluminium alloys for the automotive industry. Material Science and Engineering 2000. **A280**: p. 37-49.
9. McCafferty, E., Introduction to Corrosion Science. 2010, Alexandria: Springer.
10. Shreir, L.L., R.A. Jarman, and G.T. Burstein, Corrosion: vol 1. Metal/environment reactions, vol 2. Corrosion control. 1994.
11. Wefers, K. and C. Misra, *Oxides and Hydroxides of Aluminium.* Alcoa Technical Papers, 1987. **19**.
12. *Corrosion: Fundamentals, Testing and Protection*. ASM Handbook®, ed. S.D. Cramer and B.S. Covino Jr. Vol. 13A. 2003, Materials Park, USA: ASM International®. 1-1135.
13. Axelsen, S.B. and D. Persson, *Filiform Corrosion of Aluminium - A Literature Survey*.
14. Lobry, V., S. Vandeputte, and J. Vereecken. *Influence of the Oxygen Concentration on Filiform Corrosion of Coated Aluminium Alloys*. in *EUROCORR '97*. 1997.
15. Jenkins, A.T.A. and R.D. Armstrong, *The Breakdown in the Barrier Properties of Organic Coatings due to Filiform Corrosion,*. Corrosion Science, 1996. **38**(7): p. 1147-1157.
16. Slabaugh, W.H., et al., *Filiform Corrosion of Aluminium.* Journal of Paint Technology, 1972. **44**: p. 76.
17. Eppel, K., et al., *Corrosion of metals for automotive applications in ethanol blended biofuels.* Energy Materials: Materials Science and Engineering for Energy Systems, 2008. **3**(4): p. 227-231.
18. Scholz, M. and J. Ellermeier, *Corrosion behaviour of different aluminium alloys in fuels containing ethanol under increased temperatures.* Materialwissenschaften und Werkstofftechnik, 2006. **10**: p. 842.
19. Krüger, L., et al., *Corrosion behaviour of aluminium alloys in ethanol fuels.* Journal of Materials Science, 2011: p. 1-9.
20. Yerokhin, A.L., et al., *Plasma electrolysis for surface engineering.* Surface and Coatings Technology, 1999. **122**(2-3): p. 73-93.
21. Blawert, C., et al., *Anodizing Treatments for Magnesium Alloys and Their Effect on Corrosion Resistance in Various Environments.* Advanced engineering materials, 2006. **6**(6): p. 511-533.
22. Yerokhin, A.L., et al., *Fatigue properties of Keronite® coatings on a magnesium alloy.* Surface and Coatings Technology, 2004. **182**: p. 78-84.
23. Alisch, G., D. Nickel, and T. Lampke, *Simultaneous plasma-electrolytic anodic oxidation (PAO) of Al–Mg compounds.* Surface and Coatings Technology, 2011. **206**: p. 1085-1090.

24. Blawert, C., et al., *Influence of process parameters on the corrosion properties of electrolytic conversion plasma coated magnesium alloys.* Surface and Coatings Technology, 2005. **200**: p. 68-72.
25. http://aluminium.matter.org.uk/content/html/eng/default.asp?catid=181&pageid=21444 16710. 2012-11-23, AluMatter.
26. http://keronite.com/. 2011-12-20.
27. Malayoglua, U., et al., *An investigation into the mechanical and tribological properties of plasma electrolytic oxidation and hard-anodized coatings on 6082 aluminum alloy.* Material Science and Engineering A, 2011. **528**: p. 7451-7460.
28. Curran, J.A. and T.W. Clyne, *Thermo-physical properties of plasma electrolytic oxide coatings on aluminium.* Surface and Coatings Technology, 2005. **199**: p. 168-176.
29. Agarwala, R.C., V. Agarwala, and R. Sharma, *Electroless Ni-P Based Nanocoating Technology-A Review.* Synthesis and Reactivity in Organic, Metal-Organic and Nano-Metal Chemistry, 2006. **36**: p. 493-515.
30. Sukkasi, S., et al., *Electroless Ni-based coatings for biodiesel containers.* Journal of Coatings Technology Research, 2011. **8**(1): p. 141-147.
31. Tomlinson, W.J. and M. Girardi, *Cavitation wear of electroless nickel in distilled water and 3% NaCl water.* Surface and Coatings Technology, 1987. **31**(3): p. 213-222.
32. http://www.brinkfornickling.se. 2011-12-22.
33. Salvago, G., G. Fumagalli, and F. Brunella, *Corrosion behaviour of electroless Ni-P coatings in chloride-containing environments.* Surface and Coatings Technology, 1989. **37**(4): p. 449-460.
34. Tomlinson, W.J. and M.W. Carroll, *Substrate roughness, deposit thickness and the corrosion of electroless nickel coatings.* Journal of Materials Science, 1990. **25**(12): p. 4972-4976.
35. Kumar, S., N. Singh, and R. Prasad, *Anhydrous ethanol: A renewable source of energy.* Renewable and Sustainable Enery Reviews, 2010. **14**: p. 1830-1844.
36. Hoekman, K.S., *Biofuels in the U.S. - Challenges and Opportunities* Renewable Energy, 2009. **34**: p. 14-22.
37. Black, F., *An Overview of the Technical Implications of Methanol and Ethanol as Highway Motor Vehicle Fuels.* SAE Technical Paper, 1991. **912413**.
38. Al-Asheh, S., F. Banat, and A.A. Fara, *Dehydration of ethanol-water azeotropic mixture by adsorption through phillipsite packed-column.* Separation Science and Technology, 2009. **44**(13): p. 3170-3188.
39. Meloan, C.E., *Chemical Separations: Principles, Techniques, and Experiments*. 1999, Manhattan, Kansas: John Wiley & Sons In.
40. Horsley, L.H., *Azeotropic data*. 1952, Washington D.C: American Chemical Society.
41. Barr-David, F. and B.F. Dodge, *Vapor-liquid equilibrium at high pressures: The systems ethanol-water and 2-propanol-water.* Journal of Chemical and Engineering Data, 1959. **4**(2): p. 107-121.
42. Hughes, K., *Treatise on Alcohol-Blended Gasoline: Phase Separation and Alcohol Monitors*, Central Illinois Manufacturing Company.
43. Chen, Z.-h., et al., *Prediciotn of Vapor-Liquid Equilibrium at High Pressure Using a New Excess Free Energy Mixing Rule Coupled with the Original UNIFAC Method and the SRK Equation of State.* Industrial and Engineering Chemistry, 2009. **48**: p. 6836-6845.
44. Tochigi, K., *Prediction of High-Pressure Vapor-Liquid Equilibria.* Fluid Phase Equilibria, 1995. **104**: p. 253-260.
45. Soria, T.M., et al., *Modeling alcohol + water + hydrocarbon mixtures with the group contribution with association equation of state GCA-EoS.* Fluid Phase Equilibria, 2010. **296**: p. 116-124.
46. Volpato Filho, O., *Gasoline C made with Hydrous Ethanol*, Delphi South America Technical Center: Brazil.
47. Novitskiy, A.A., et al., *A New Continous Method for Performing Rapid Phase Equilibrium Measurements on Binary Mixtures Containing CO2 or H2O at High*

Pressures and Temperatures. Journal of Chemical and Engineering Data, 2009. **54**: p. 1580-1584.
48. Orbey, H., S.I. Sandler, and D.S.H. Wong, *Accurate equation of state predictions at high temperatures and pressures using the existing UNIFAC model.* Fluid Phase Equilibria, 1993. **85**: p. 41-54.
49. Tokunaga, J., *Solubilities of Oxygen, Nitrogen, and Carbon Dioxide in Aqueus Alcohol Solutions.* Journal of Chemical and Engineering Data, 1975. **20**(1): p. 41-46.
50. Korotney, D., *Water Phase Separation in Oxygenated Gasoline - Corrected version of Kevin Krause memo*.
51. Weber de Menezes, E., et al., *Addition of an azeotropic ETBE/ethanol mixture in eurosuper-type gasolines.* Fuel, 2006. **85**: p. 2567-2577.
52. Johansen, T. and J. Schramm, *Low-temperature miscibility of ethanol-gasoline-water blends in flex fuel applications.* Energy Sources, Part A: Recovery, Utilization and Environmental Effects, 2009. **31**(18): p. 1634-1645.
53. Yoo, Y.H., et al., *Corrosion characteristics of aluminium alloy in bio-ethanol blended gasoline fuel: Part 1. The corrosion properties of aluminium alloy in high temperature fuels.* Fuel, 2011. **90**.
54. Letcher, T.M., et al., *Ternary phase diagrams for gasoline-water-alcohol mixtures.* Fuel, 1986. **65**(7): p. 891-894.
55. Fabrikant, I.I. and H. Hotop, *On the validity of the Arrhenius equation for electron attachment rate coefficients.* Journal of Chemical Physics, 2008. **128**(12).
56. Kaufmann, H., et al., *Korrosion durch Biokraftstoffe - Schutz durch Beschichtungen auch bei zyklischer Beanspruchung auch bei zyklischer Beanspruchung.* Materialwissenschaft und Werkstofftechnik, 2006. **37**(12): p. 983-993.
57. Günzler, H., *IR Spectroscopy*. 2002, Weinheim: Wiley-VCH Verlag GmbH & Co.
58. *Failure Analysis and Prevention.* ASM Handbook. , ed. W.T. Becker and R.J. Shipley. Vol. 11. 2003, ASM International®: Materials Park, USA. 1-1164.
59. http://www.purdue.edu/rem/rs/sem.htm. 2012.
60. Bruttel, P. and R. Schlink, *Water Determination by Karl Fischer Titration* 2003, Metrohm Monograph: Herisau, Switzerland. p. 1-80.
61. http://www.machinerylubrication.com/Read/594/karl-fischer-coulometric-titration. 2010-10-12.
62. Nilsson, J.-O. 2012, Sapa Technology: Finspång.
63. http://klimakamra.hu/files/2813/1534/7265/WT_WK_Ex_E.pdf. 2011-12-10.
64. Talus, A., *NKM*. 2010.
65. Öhman, M. and D. Persson, *An integrated in situ ATR-FTIR and EIS set-up to study buried metalâ€“polymer interfaces exposed to an electrolyte solution.* Electrochimica Acta, 2007. **52**(16): p. 5159-5171.
66. Socrates, G., *Infrared Characteristic Group Frequencies*. 1997, Chippenham, England: John Wiley & Sons Ltd. 249.
67. Persson, D. 2012, Swerea KIMAB: Stockholm.

11 Appendix

11.1 Appendix I

Alcoholate corrosion water dependency testing carried out by Annika Talus at Swerea KIMAB.

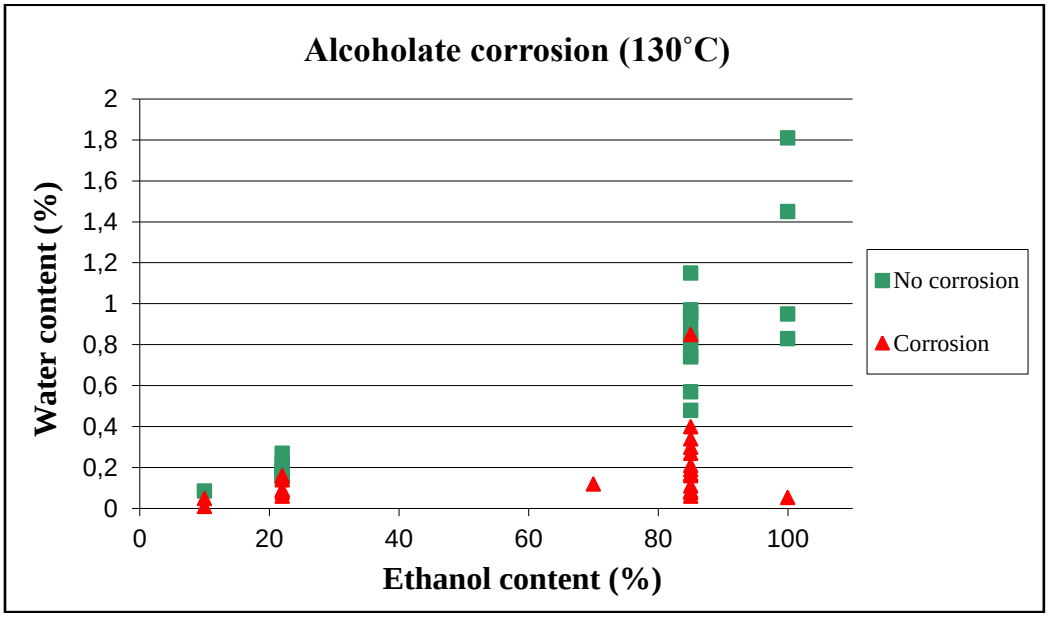

11.2 Appendix II

The results from the oxygen pressurisation on aluminium alloy AA6063 are summarised

Pressurisation with oxygen on material AA6063 contact with liquid and gas									
			Initial pressure (bar)								
			1	6	11	1	6	11	1	6	11
Test 1											
T=120°C, T=96h											
Final pressure			1	1	1	1	1	1	1	1	1
Corrosion			x	-	-	-	-	x	-	-	-
Water content (%)	Start	0.16									
	End		-	2.14	2.95	0.31	2.21	-	0.30	2.16	2.94
Test 2											
T=130°C, T=24h											
Final pressure			1	1	4	1	1	1	1	1	1
Corrosion			x	-	-	-	-	-	x	-	-
Water content (%)	Start	0.14									
	End		-	1.59	3.70	0.34	2.51	1.73	-	2.89	3.77
Test 3											
T=150°C, T=12h											
Final pressure			1	1	1	1	1	2	1	1	6
Corrosion			x	x	-	x	-	-	x	-	-
Water content (%)	Start	0.24									
	End		-	-	3.38	-	2.60	4.75	-	2.62	0.59

Test 4											
T=125°C, T=36h											
Final pressure			1	1	2	1	1	3	1	1	3
Corrosion			-	-	-	x	-	-	-	-	-
Water content (%)	Start	0.18									
	End		0.35	-	3.98	-	-	-	0.45	-	-
Test 5											
T=140°C, T=24h											
Final pressure			1	1	2	1	1	2	1	1	3
Corrosion			x	-	-	x	-	-	x	-	-
Water content (%)	Start	0.18									
	End		-	3.17	3.44	-	3.18	4.51	-	2.63	3.97
Test 6											
T=125°C, T=72h											
Final pressure			1	1	1						
Corrosion			x	-	-						
Water content (%)	Start	0.25	0								
	End		-	-	-						
Test 7											
T=135°C, T=54h											
Final pressure			1	1	4	1	1	4	1	2	3
Corrosion			x	-	-	x	-	-	-	-	-
Water content (%)	Start	0.17									
	End		-	2.60	-	-	2.35	3.66	0.32	2.70	3.06
Test 8											
T=145°C, T=18h											
Final pressure			1	1	2						
Corrosion			x	-	-						
Water content (%)	Start	0.17									
	End		-	1.73	-						

The result from the oxygen pressurisation on AA6063 samples above the solution.

Pressurisation with oxygen on material AA6063 above solution					
			Initial pressure (bar)		
			1	6	11
Test 1					
T=120°C, T=96h					
Final pressure			1	1	1
Corrosion			-	-	-
	Start	0.16			
	End		0.33	1.96	4.39
Test 2					
T=130°C, T=24h					
Final pressure			1	1	1
Corrosion			x	-	-
Water content (%)	Start	0.14	-0.01		
	End		-	2.36	1.7
Test 3					
T=150°C, T=12h					
Final pressure			1	1	1
Corrosion			x	x	-
Water content (%)	Start	0.24			
	End		-0.01	-	-

Test 4					
T=125°C, T=36h					
Final pressure			1	1	1
Corrosion			-	-	-
Water content (%)	Start	0.18			
	End		0.36	-	-
Test 5					
T=140°C, T=24h					
Final pressure			1	1	1
Corrosion			x	-	-
Water content (%)	Start	0.18			
	End		-	3.56	4.56

The result from the oxygen pressurisation on AA6063 samples in the solution.

Pressurisation with oxygen on material AA6063 in solution					
			Initial pressure (bar)		
			1	6	11
Test 1					
T=120°C, T=96h					
Final pressure			1	1	1
Corrosion			-	-	-
Water content (%)	Start	0,16			
	End		0.33	2.34	3.33
Test 2					
T=130°C, T=24h					
Final pressure			1	1	1
Corrosion			x	-	-
Water content (%)	Start	0.14			
	End			2.16	2.88
Test 3					
T=150°C, T=12h					
Final pressure			1	1	4
Corrosion			x	x	x
Water content (%)	Start	0.24			
	End		-	2.84	-

Increase of water from the oxygen pressurisation tests.

Initial pressure (bar)	**Increase of water (%)**
1	95
6	1459
11	1863

The results from the pressurisation test with nitrogen using samples of aluminium alloy AA6063 is presented.

Pressurisation with nitrogen on material AA6063 contact with liquid and gas					
			Initial pressure (bar)		
			1	6	11
Test 9					
T=100°C, T=24h					
Final pressure			1	5	9
Corrosion			-	-	-
Water content (%)	Start	0.3			
Test 10					
T=(100+) 100°C, T=(24+) 72h					
Final pressure			1	6	11
Corrosion			-	-	-
Water content (%)	Start	-			
Test 11					
T=100°C, T=72h					
Final pressure			1	5	10
Corrosion			-	-	-
Water content (%)	Start	0.3			
Test 12					
T=120°C, T=36h					
Final pressure			-	-	-
Corrosion			-	x	x
Water content (%)	Start	0.06			
		End	0.15		
Test 13					
T=120°C, T=36h					
Final pressure			-	-	-
Corrosion			-	-	-
Water content (%)	Start	0.32			
		End	0.41	0.33	0.32
Test 14					
T=130°C, T=12h					
Final pressure			1	4	9
Corrosion			-	-	-
Water content (%)	Start	0.27			
Test 15					
T=130°C, T=24h					
Final pressure			-	-	9
Corrosion			x	x	-
Water content (%)	Start	0.3			

The results from the pressurisation tests with nitrogen using samples of A380:

Pressurisation with nitrogen on material A380 contact with liquid and gas					
			Initial pressure (bar)		
			1	6	11
Test 16					
T=100°C, t=3h					
Final pressure			1	5	10
Corrosion			-	-	-
Water content (%)	Start	0.3			
Test 17					
T=(100+) 100°C, t=(3+) 24h					
Final pressure			1	1	1
Corrosion			-	-	-
Water content (%)	Start	-			
Test 18					
T=(100+100+) 130°C					
t=(3+24+) 12h					
Final pressure			-	-	-
Corrosion			x	x	x
Water content (%)	Start	0.27			
Test 19					
T=100°C, t=72h					
Final pressure			1	5	13
Corrosion			x	-	x
Water content (%)	Start	0.3			

Pressurisation with nitrogen on material A380 above solution					
			Initial pressure (bar)		
			1	6	11
Test 17					
T=100°C, t=3h					
Final pressure			1	6	9
Corrosion			-	-	-
Water content	Start	0.3			
Test 18					
T=(100+) 100°C, t=(3+) 24h					
Final pressure			1	5	9
Corrosion			-	-	-
Water content	Start	-			
Test 19					
T=(100+100+) 130°C					
t=(3+24+) 12h					
Final pressure			1	5	10
Corrosion			-	-	x
Water content	Start	0.27			
Test 20					
T=100°C, t=72h					
Final pressure			1	4	9
Corrosion			-	-	-
Water content	Start	0.3			

Material A380 in solution					
			Initial pressure (bar)		
			1	6	11
Test 21					
T=100°C, t=3h					
Final pressure			1		
Corrosion			x		
Water content	Start	0.3			

11.3 Appendix III

No corrosion		Corrosion	
Temperature	**Time (h)**	**Temperature**	**Time (h)**
100	24	120	96
100	72	125	36
120	12	125	72
120	96	130	9
120	96	130	21
120	96	130	23
120	96	130	25
125	36	130	27
125	36	140	21
125	36	140	23
130	24	140	25
130	24	140	27
130	24	150	2
		150	8
		150	10
		150	12
		150	14
		150	16
		145	18
		135	52
		135	56